RNA
A PUBLICATION OF THE RNA SOCIETY

Stalling of spliceosome assembly at distinct stages by small-molecule inhibitors of protein acetylation and deacetylation

Andreas N. Kuhn, Maria A. van Santen, Andreas Schwienhorst, et al.

RNA 2009 15: 153-175 originally published online November 24, 2008
Access the most recent version at doi:10.1261/rna.1332609

Stalling of spliceosome assembly at distinct stages by small-molecule inhibitors of protein acetylation and deacetylation

ANDREAS N. KUHN,[1] MARIA A. VAN SANTEN,[1] ANDREAS SCHWIENHORST,[2] HENNING URLAUB,[3] and REINHARD LÜHRMANN[1]

[1]Department of Cellular Biochemistry, Max Planck Institute for Biophysical Chemistry, D-37077 Göttingen, Germany
[2]Department of Molecular Genetics and Preparative Molecular Biology, Institute for Microbiology and Genetics, D-37077 Göttingen, Germany
[3]Bioanalytical Mass Spectrometry Group, Max Planck Institute for Biophysical Chemistry, D-37077 Göttingen, Germany

ABSTRACT

The removal of intervening sequences from a primary RNA transcript is catalyzed by the spliceosome, a large complex consisting of five small nuclear (sn) RNAs and more than 150 proteins. At the start of the splicing cycle, the spliceosome assembles anew onto each pre-mRNA intron in an ordered process. Here, we show that several small-molecule inhibitors of protein acetylation/deacetylation block the splicing cycle: by testing a small number of bioactive compounds, we found that three small-molecule inhibitors of histone acetyltransferases (HATs), as well as three small-molecule inhibitors of histone deacetylases (HDACs), block pre-mRNA splicing in vitro. By purifying and characterizing the stalled spliceosomes, we found that the splicing cycle is blocked at distinct stages by different inhibitors: two inhibitors allow only the formation of A-like spliceosomes (as determined by the size of the stalled complexes and their snRNA composition), while the other compounds inhibit activation for catalysis after incorporation of all U snRNPs into the spliceosome. Mass-spectrometric analysis of affinity-purified stalled spliceosomes indicated that the intermediates differ in protein composition both from each other and from previously characterized native A and B splicing complexes. This suggests that the stalled complexes represent hitherto unobserved intermediates of spliceosome assembly.

Keywords: pre-mRNA splicing; spliceosome; proteomics; histone deacetylase/HDAC; histone acetyltransferase/HAT

INTRODUCTION

Pre-mRNA splicing, the removal of introns from the primary RNA transcript, is an essential process in the biosynthesis of mature mRNAs in eukaryotic cells. Most genes in higher eukaryotes contain more than one intron, which provides the possibility to remove various combinations of introns from a single pre-mRNA; this choice is referred to as alternative splicing. The majority of the human genes are spliced in this way, which seems to be the main source of proteomic complexity in humans (Hastings and Krainer 2001; Blencowe 2006). Furthermore, it has been estimated that ~15% of all mutations that cause a genetic disease in humans lead to a failure in the correct splicing of the corresponding pre-mRNA, which disturbs the expression of the gene (Krawczak et al. 1992).

The splicing reaction occurs by a two-step transesterification mechanism. First, the 2′ hydroxyl group of a conserved adenosine nucleotide within the so-called branch-point region of the intron attacks the phosphate group at the 5′ end of the intron, the so-called 5′ splice site, which releases the 5′ exon. Subsequently, the 3′ hydroxyl group of the released 5′ exon attacks the phosphate group at the 3′ splice site for the second step; in this way, the 5′ and 3′ exons become joined, forming the mature mRNA. The entire process is catalyzed by the spliceosome, which consists of the U1, U2, U4, U5, and U6 small nuclear ribonucleoprotein particles (snRNPs) and numerous additional non-snRNP proteins (Will and Lührmann 2006). Each U snRNP contains its corresponding U snRNA, a common set of seven Sm proteins (or seven LSm proteins in the case of the U6 snRNP), and additional particle-specific proteins. The spliceosome is a highly dynamic machinery that assembles anew onto each intron to be

Reprint requests to: Reinhard Lührmann, Department of Cellular Biochemistry, Max Planck Institute for Biophysical Chemistry, Am Fassberg 11, 37077 Göttingen, Germany; e-mail: reinhard.luehrmann@mpi-bpc.mpg.de; fax: 49-551-201-1197.

Article published online ahead of print. Article and publication date are at http://www.rnajournal.org/cgi/doi/10.1261/rna.1332609.

excised, in an ordered process involving distinct intermediate spliceosomal complexes.

The pre-mRNA is first recognized by the U1 snRNP in an ATP-independent manner to form the spliceosomal E complex, which involves base-pairing of the U1 snRNA to the 5′ splice site. In addition, the U2 snRNP is loosely associated with the pre-mRNA in the E complex. The ATP-dependent, stable binding of the U2 snRNP to the branch-point region—guided in part by base-pairing between the U2 snRNA and the branch-point region—leads to the formation of the A complex. The U4, U5, and U6 snRNPs are added to the A complex as a preformed U4/U6•U5 tri-snRNP, in which the U4 and U6 snRNAs are base-paired to each other. This leads to formation of the spliceosomal B complex, which—despite the presence of all five U snRNPs—still represents a pre-catalytic entity that has to be activated. Activation of the spliceosome for catalysis is accompanied by release of the U1 snRNA from the 5′ splice site and unwinding of the U4/U6 snRNAs, which destabilizes the binding of the U1 and U4 snRNPs to the spliceosome. Thus, the so-called activated spliceosomal B* complex contains only the U2, U5, and U6 snRNAs, which now form an intricate base-paired network with the pre-mRNA. The first transesterification reaction is accompanied by the formation of the spliceosomal C complex. After the second catalytic step, the spliceosome dissociates, releasing the products of the splicing reaction, and the U snRNPs are recycled for another round of splicing catalysis.

While the assembly of the spliceosome is quite well understood at the RNA level, it has only recently become clear that the dynamic nature of the spliceosome is also reflected by changes in the protein composition that go far beyond the addition and release of the proteins of the individual U snRNPs. This was first recognized as a result of proteomic studies of the known intermediates of spliceosome assembly as described above. By now, several laboratories have purified various human splicing complexes and determined their protein composition by mass spectrometry (Hartmuth et al. 2002; Jurica et al. 2002; Makarov et al. 2002; Rappsilber et al. 2002; Zhou et al. 2002; Makarova et al. 2004; Deckert et al. 2006; Behzadnia et al. 2007; Bessonov et al. 2008). While this has increased the number of known splicing factors, the detailed hierarchy of assembly—i.e., order of recruitment, interdependence between different factors, and signals for release of spliceosomal proteins—is only poorly understood (Jurica and Moore 2003).

Sequence homology has revealed that numerous proteins associated with the spliceosome possess potential enzymatic activities. These include DExD/H-type RNA-dependent ATPases and RNA helicases, peptidyl-prolyl *cis*/*trans* isomerases, and protein kinases (Staley and Guthrie 1998). It is therefore plausible that such activities might act on RNA and protein conformations, or on post-translational modification states of proteins, during the splicing cycle. However, the function of a large number of the enzymes in the spliceosome remains to be established. Given that many of these enzymes are likely to be involved in at least one conformational switching event, more spliceosome maturation states must exist than the limited number of intermediates so far identified. Logical extension of this argument would imply that the blocking of individual enzyme activities could stall the spliceosome at novel intermediate stages and thus be a useful tool for probing its maturation and catalytic activity. If successful, this could lead to finer resolution of the stages through which the spliceosome passes during the splicing cycle.

The study of the ribosome has been greatly facilitated by the use of antibiotics, which block translation at specific steps and thus allow a detailed characterization of these intermediates. Small-molecule inhibitors of pre-mRNA splicing could in the same way be very helpful for mechanistic studies. Only recently it was shown for the first time that two naturally occurring compounds, FR901464 and pladienolide, specifically inhibit the splicing of pre-mRNA (Kaida et al. 2007; Kotake et al. 2007). In an earlier study, Soret et al. (2005) reported the identification of indole derivatives that target SR proteins and thereby influence alternative splicing. Similarly, it was found that cardiotonic steroids modulate alternative splicing (Stoilov et al. 2008). To our knowledge, none of these few small-molecule inhibitors of pre-mRNA splicing have been used to isolate the stalled splicing complexes for further analysis, such as the determination of protein composition by mass spectrometry. However, it is reasonable to assume that such compounds would allow the specific enrichment of known or even previously unknown intermediates of the pre-mRNA splicing cycle, whose functional and structural characterization could then give further insight into the mechanism of spliceosome assembly and catalysis.

Post-translational modification plays an important role in the regulation of a number of biological processes, with phosphorylation the most prominent modification. In addition, proteins can be acetylated at lysine residues, and the corresponding enzymes are for historical reasons known as histone acetyltransferases (HATs) and histone deacetylases (HDACs). A number of examples of a connection between RNA processing and protein acetylation have been reported; e.g., SF3b130, a component of the SF3b complex of the 17S U2 snRNP that is also known as SAP130, is associated in HeLa cells with STAGA, a mammalian SAGA-like HAT complex (Martinez et al. 2001). It has also been reported that Sam68, an RNA-binding protein of the STAR family that has been implicated in alternative splicing (Matter et al. 2002), is acetylated in vivo, and that the acetylation state of Sam68 correlates with its ability to bind to its cognate RNA (Babic et al. 2004). Furthermore, the protein DEK, which has been shown to be required for proofreading of 3′ splice site recognition by U2AF (Soares et al. 2006), undergoes acetylation in vivo (Cleary et al. 2005). An increase in the degree of acetylation of

DEK—either by inhibition of deacetylation or by overexpression of the PCAF acetylase—results in accumulation of DEK within interchromatin granule clusters, which are subnuclear structures that contain RNA-processing factors. In addition, p68, a DExD/H-box RNA helicase that has been shown to be involved in the splicing of pre-mRNA (Liu 2002), associates with HDAC1 (Wilson et al. 2004). Finally, factors implicated in the acetylation and deacetylation of proteins have been found in purification of mixed populations of splicing complexes (Rappsilber et al. 2002; Zhou et al. 2002).

To identify small molecules that specifically block the splicing of pre-mRNA at distinct steps, we initiated a screening for inhibitors of this splicing. As a first test, we examined previously published inhibitors of protein acetylation and deacetylation for their effect, if any, on the splicing reaction in vitro. We found that pre-mRNA splicing in vitro is blocked by three structurally distinct small-molecule inhibitors of HATs and also by three small-molecule inhibitors of HDACs. While some of these compounds inhibit only in the millimolar range, others exert their effect at micromolar concentrations similar to those reported for their inhibition of HATs and HDACs. Characterization of the splicing complexes that accumulate in the presence of individual acetylation and deacetylation inhibitors on native gels, and also the identification of their RNA and protein compositions, demonstrates that spliceosome assembly is stalled at distinct stages. The stalled complexes represent functional intermediates of the splicing cycle, because they can be chased into active spliceosomes in the presence of appropriately depleted nuclear extract. Mass-spectrometric analysis of affinity-purified complexes showed that the stalled intermediates of spliceosome assembly differ in their protein composition, both from each other and from previously characterized native splicing complexes (i.e., those purified in the absence of any inhibitor). This evidence suggests that we have identified previously unobserved intermediates of spliceosome assembly.

RESULTS

Blockage of pre-mRNA splicing before catalysis by inhibitors of protein deacetylation

We investigated a number of known bioactive compounds for possible inhibitory effect on the splicing in vitro of MINX pre-mRNA. Earlier work had identified the presence of histone deacetylases (HDACs) in purifications of mixed populations of spliceosomes (Rappsilber et al. 2002; Zhou et al. 2002). HDACs catalyze the deacetylation of the ε-amino group of acetylated lysine residues not only in histones, but in a multitude of proteins (Kouzarides 2000; Grozinger and Schreiber 2002; Yang 2004). Therefore, we chose suberoylanilide hydroxamic acid (SAHA) (Fig. 1A), a well-known inhibitor of the Zn^{2+}-dependent classes of histone deacetylases (HDAC classes I and II) (Hildmann et al. 2007), as one of the compounds to test. We observed a dose-dependent inhibition of pre-mRNA splicing in vitro in the presence of SAHA, but not DMSO, the solvent used for the compound (Fig. 1B, lanes 2–7). As in the absence of any inhibitor the splicing reaction already reaches a plateau after ~30 min (data not shown), the inhibition of pre-mRNA splicing up to 90 min indicates that the reaction is essentially blocked and not merely slowed down. SAHA interfered with the formation of both the products (mature mRNA and excised lariat-intron) and the intermediates (5′-exon and lariat-intron/3′-exon) of the reaction, demonstrating that in this case pre-mRNA splicing is blocked before the first catalytic step.

Quantification of the splicing efficiency demonstrated that SAHA inhibits pre-mRNA splicing with an IC_{50} (concentration giving 50% inhibition) of ~1.5 mM. This is three orders of magnitude higher than the reported values for HDAC inhibition by SAHA (Table 1). Therefore, to confirm the specificity of this inhibition, we tested two derivatives that resemble SAHA but are inactive in HDAC inhibition: suberoylanilide (SA) and suberoyl bis-hydroxamic acid (SBHA) (Fig. 1A). SA has a carboxylic acid in place of the hydroxamic acid, which is essential for inhibition of HDACs. In contrast, SBHA contains two hydroxamic acid groups, but lacks the anilide entity. The latter serves as a control that the inhibition observed is not simply due to any hydroxamic acid, but depends on the context of the whole molecule, as observed for inhibition of deacetylation. In addition, these compounds are also a control that the effect observed is not simply due to aggregation of one or more essential splicing factor, but rather based on specific binding. At the concentrations where SAHA had been found to inhibit splicing, both SA and SBHA failed to show inhibition (Fig. 1B, lanes 8–17), supporting the specificity of inhibition observed with SAHA. Furthermore, we investigated three additional HDAC inhibitors related to SAHA, namely, MS-275 (Saito et al. 1999), scriptaid (Su et al. 2000), and trichostatin A (Yoshida et al. 1990), all of which belong to the group of hydroxamic acids and hydroxamic esters. MS275, scriptaid, and trichostatin A all inhibit pre-mRNA splicing in vitro (Table 1). The concentrations required for inhibition of pre-mRNA splicing are again about a thousand times higher than values reported for HDAC inhibition (Table 1). Thus, pre-mRNA splicing is inhibited by small molecules containing a hydroxamic acid group in a specific context similar to the one required for HDAC inhibition, but with considerably higher IC_{50} values.

The class III HDACs—also called sirtuins, a term based on the founding member, the yeast Sir2 protein—use a deacetylation mechanism fundamentally different from that of the HDAC classes I and II; their activity depends on NAD as a cofactor (Imai et al. 2000; Landry et al. 2000b). We investigated whether four previously identified chemicals that inhibit NAD-dependent deacetylases—dihydrocoumarin

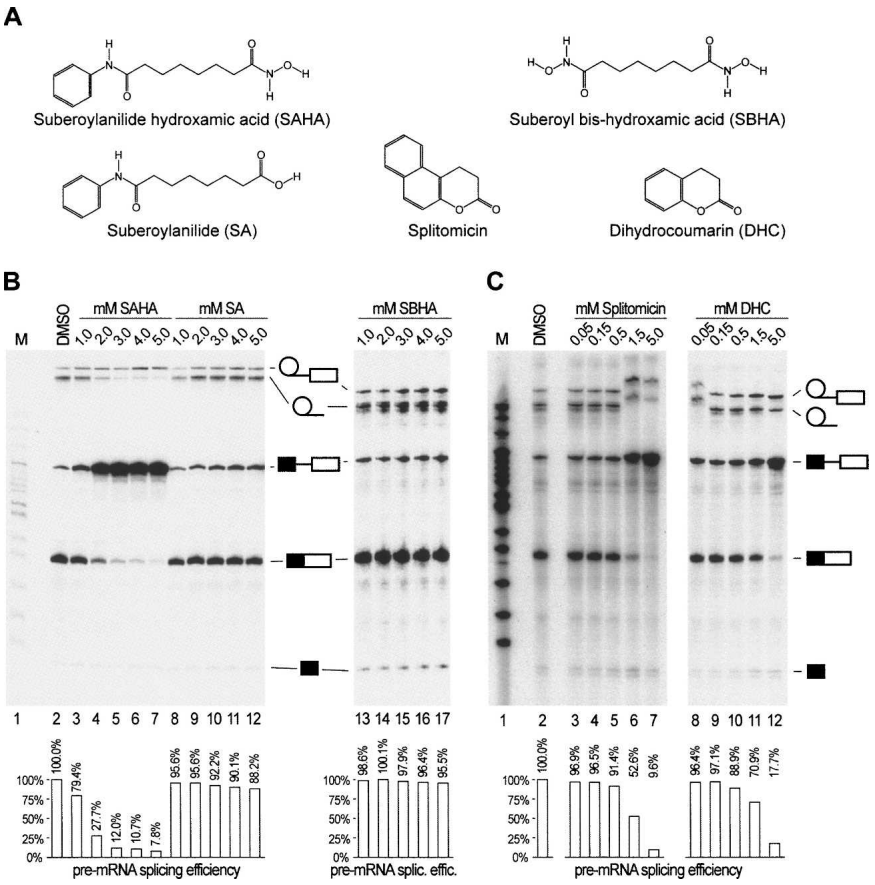

FIGURE 1. Blockage of pre-mRNA splicing before the first catalytic step by inhibitors of protein deacetylases. (*A*) Structures of suberoylanilide hydroxamic acid (SAHA), an inhibitor of HDAC classes I and II, two derivatives thereof—suberoylanilide (SA) and suberoylanilide bis-hydroxamic acid (SBHA)—and the HDAC class III inhibitors dihydrocoumarin (DHC) and splitomicin. (*B*) Increasing concentrations (as indicated *above* the lanes) of (lanes *3–7*) SAHA, (lanes *8–12*) SA, and (lanes *13–17*) SBHA were tested for their effect on the splicing in vitro of ^{32}P-labeled MINX pre-mRNA. After splicing, the radiolabeled RNA was analyzed by denaturing PAGE followed by autoradiography. The positions of lariat-intron/3′-exon, lariat-intron, pre-mRNA, fully spliced mRNA, and 5′-exon (*top* to *bottom*) are indicated *between* lanes *12* and *13*. (Lane *1*) M, size marker; (lane *2*) control reaction with DMSO, the solvent used for the small-molecule inhibitors. The splicing efficiency is shown *below* each lane. (*C*) Increasing concentrations of (lanes *3–7*) splitomicin and (lanes *8–12*) DHC. Other details are as in *B*. (Note that the different migration observed for the lariat-intron/3′-exon and lariat-intron observed in lanes *6–8* has only been observed in the one experiment shown here, and thus is apparently an artifact.)

(DHC) (Fig. 1A; Olaharski et al. 2005), nicotinamide (Landry et al. 2000a; Luo et al. 2001), sirtinol (Grozinger et al. 2001), and splitomicin (Fig. 1A; Bedalov et al. 2001)—affect the splicing reaction in vitro. As can be seen in Figure 1C, splicing of the MINX pre-mRNA is blocked by increasing concentrations of splitomicin and DHC. In contrast, nicotinamde and sirtinol have no effect on pre-mRNA splicing in vitro (Table 1). No significant accumulation of the splicing intermediates, the 5′-exon and lariat-intron/3′-exon, could be observed at inhibitory concentrations of either splitomicin or DHC, indicating that these two compounds again block pre-mRNA splicing before the first catalytic step. Splitomicin gave slightly stronger inhibition, with an IC_{50} of 1.5 mM, than DHC, with an IC_{50} of 2.0 mM (Fig. 2A; Table 1). Thus, we have shown that diverse inhibitors of protein deacetylation—targeting different classes of HDAC enzymes—block pre-mRNA splicing before catalysis.

Blockage of pre-mRNA splicing before catalysis by Inhibitors of protein acetylation

Next, we tested three previously identified small-molecule inhibitors of histone acetyltransferases (HATs)—the enzymes that catalyze the acetylation of proteins—for their effect on the splicing in vitro of MINX pre-mRNA. One of the compounds chosen, butyrolactone 3 (BA3) (Fig. 2A), shows specificity toward Gcn5/PCAF-type acetyltransferases (Biel et al. 2004). In contrast, anacardic acid (AA) and garcinol (Fig. 2A) have been reported to be acetyltransferase inhibitors with similar potency for both the p300/CBP and Gcn5/PCAF families of HATs (Balasubramanyam et al. 2003, 2004). As can be seen in Figure 2B, increasing concentrations of the HAT inhibitors also interfered with pre-mRNA splicing in vitro. As observed for the HDAC inhibitors, the reaction was blocked before the first catalytic step, as neither the products of the reaction (mature mRNA and excised lariat-intron) nor its intermediates (5′-exon and lariat-intron/3′-exon) were observed upon inhibition. With IC_{50} values of 50 μM and 25 μM for AA and garcinol, respectively, the two compounds were found to be stronger inhibitors of pre-mRNA splicing than BA3 (IC_{50} of 0.5 mM). Intriguingly, for all three compounds, IC_{50} values for inhibition of splicing are of the same order of magnitude as those for HAT inhibition (Table 1).

In summary, we have identified six small molecules as novel inhibitors of pre-mRNA splicing, all of which block splicing before the first catalytic steps.

HAT and HDAC inhibitors affect both U2- and U12-dependent splicing pathways

To verify that the effect on pre-mRNA splicing observed with the acetyltransferase and deacetylase inhibitors is not

TABLE 1. HAT and HDAC inhibitors used in this study

Compound	Known inhibitor of	With IC_{50} of	IC_{50} (pre-mRNA splicing)
SAHA	Zn^{2+}-dependent HDACs (HDAC classes I and II)	0.01–4 μM	1.5 mM
MS-275	Zn^{2+}-dependent HDACs (HDAC classes I and II)	5–10 μM	0.5 mM
Scriptaid	Zn^{2+}-dependent HDACs (HDAC classes I and II)	0.06–1 μM	0.9 mM
Trichostatin A	Zn^{2+}-dependent HDACs (HDAC classes I and II)	0.6–490 nM	1.0 mM
DHC	NAD-dependent HDACs (HDAC class III)	30–250 μM	2.0 mM
Nicotine amide	NAD-dependent HDACs (HDAC class III)	100 μM	No inhibition up to 10 mM
Sirtinol	NAD-dependent HDACs (HDAC class III)	75 μM	No inhibition up to 5 mM
Splitomicin	NAD-dependent HDACs (HDAC class III)	100 μM	1.5 mM
BA3	HATs (Gcn5/PCAF family)	0.5 mM	0.5 mM
AA	HATs (p300/CBP and Gcn5/PCAF families)	5–10 μM	50 μM
Garcinol	HATs (p300/CBP and Gcn5/PCAF families)	5–7 μM	25 μM

Listed are all the compounds used in this study, the enzyme classes for which these are known to be inhibitors, the reported IC_{50} values for this inhibition (concentration that gives 50% inhibition; see main text for citations), and the IC_{50} values for pre-mRNA splicing as determined here.

specific for the substrate used, we conducted similar tests on the splicing in vitro of a different pre-mRNA, β-globin. The splicing of β-globin pre-mRNA was found to be inhibited before the first catalytic step by concentrations of the HAT and HDAC inhibitors similar to those observed to inhibit the splicing of MINX pre-mRNA (data not shown). In addition, we investigated whether splicing of p120 pre-mRNA, which is spliced by the U12-dependent spliceosome, also is blocked by these compounds in vitro. As shown in Figure 3, we observed that splicing of p120 pre-mRNA by the minor spliceosome is also inhibited by AA, BA3, garcinol, SAHA, splitomicin, and DHC before catalysis, but was unaffected in control reactions containing only DMSO. Altogether, these results demonstrate clearly that the newly identified inhibitors generally interfere with pre-mRNA splicing in vitro.

Blockage of the splicing cycle at distinct stages by different inhibitors

To determine at what point during spliceosome assembly and activation the reaction is blocked by these novel inhibitors of pre-mRNA splicing, we analyzed splicing-complex formation in the presence of the compounds by native gel electrophoresis. Splicing reactions were performed in the presence of inhibitory concentrations of SAHA, splitomicin, DHC, AA, BA3, or garcinol, stopped at different time points, and loaded onto a native gel (Fig. 4). Because of the structural and functional similarities of the hydroxamic acid-based inhibitors, we chose SAHA as a representative member of this group for further studies.

In the absence of any inhibitor, but with DMSO (Fig. 4A,B, lanes 1–5), mainly A complex was observed after 2 min. After 7 min, maximum amounts of B complex were formed at the expense of A complex. After 20 min, the amount of complex A had decreased substantially, and that of complex B was also reduced; after 60 min, both complexes had reacted to completion, and, accordingly, the mRNP complex was observed. Owing to the fast completion of the two steps of the splicing reaction with MINX pre-mRNA, complex C could not be detected, as previously observed (Das and Reed 1999).

In the presence of SAHA (Fig. 4A, lanes 6–10), splitomicin (Fig. 4A, lanes 11–15), DHC (Fig. 4A, lanes 16–20), or BA3 (Fig. 4B, lanes 11–15), the formation of B complexes was essentially indistinguishable from the control reaction for the first 20 min of incubation. However, the decrease in amounts of the B complexes was reduced significantly in the presence of these compounds, and the formation of mRNPs after 60 min, seen in the DMSO control, was no longer observed. This indicates that the splicing reaction is blocked by SAHA, splitomicin, DHC, and BA3 after assembly of a complete spliceosome, but before its activation. Some decline in the amount of B complexes was seen between 20 and 60 min, with varying degrees for SAHA, splitomicin, DHC, and BA3. The

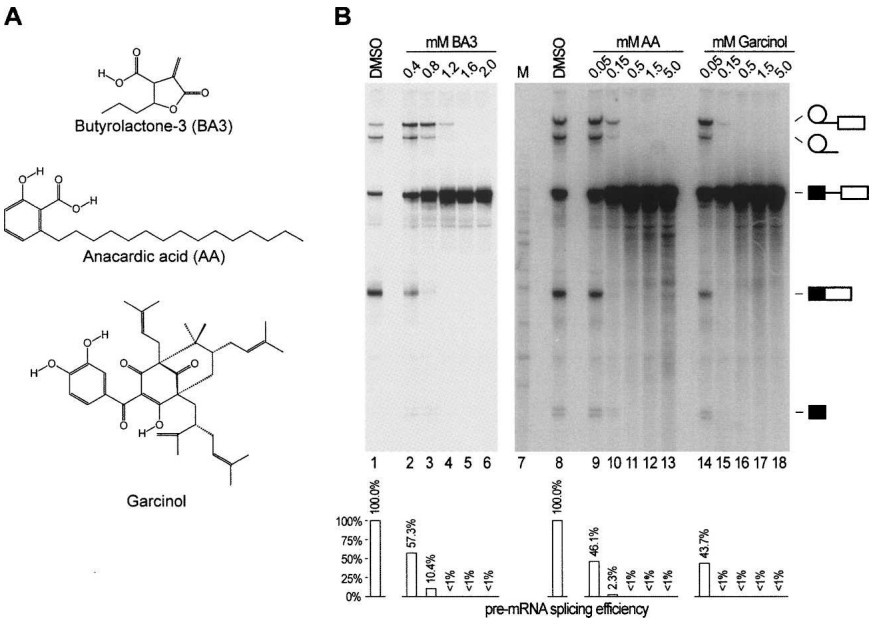

FIGURE 2. Blockage of pre-mRNA splicing before the first catalytic step by inhibitors of protein acetylation. (*A*) Structures of the HAT inhibitors butyrolactone 3 (BA3), anacardic acid (AA), and garcinol. (*B*) Increasing concentrations (as indicated *above* the lanes) of (lanes *2–6*) BA3, (lanes *9–13*) AA, and (lanes *14–18*) garcinol were tested for their effect on the efficiency of the splicing of ^{32}P-labeled MINX pre-mRNA in vitro. After the reaction, the radiolabeled RNA was analyzed by denaturing PAGE followed by autoradiography. The positions of lariat-intron/3′-exon, lariat-intron, pre-mRNA, fully spliced mRNA, and 5′-exon (*top* to *bottom*) are indicated on the *right*. (Lanes *1*,*8*) Control reaction with the solvent DMSO; (lane *7*) M, size marker. The splicing efficiency is shown *below* each lane.

disappearance of B complexes over time was most probably due to a combination of incomplete inhibition of pre-mRNA splicing with the inhibitor concentrations used, and disintegration of inactive spliceosomes.

In contrast, no B complex could be observed in the presence of AA (Fig. 4B, lanes 6–10). Instead, the A complex, the formation of which after 2 min was slightly reduced compared with the control reaction, reached a maximum level after 7 min and then remained stable for the remaining incubation period. This indicates either that the pre-mRNA splicing cycle is blocked by AA before the formation of the B complex, or that AA destabilizes complex B after its formation. Similarly to the result with AA, no B complex (or no stable B complex) was assembled in the presence of garcinol (Fig. 4A, lanes 16–20). However, while the A complex accumulated to a high level in the presence of AA, only a small amount of A complex—which even disappears later in the incubation—was formed in the presence of garcinol. This suggests that the A complex assembled in the presence of garcinol is not as stable as the A complex that is stalled by AA. Nevertheless, sufficient amounts of complex A for further characterization could be isolated (see below). Altogether, these results show that the novel small-molecule inhibitors of pre-mRNA splicing block the reaction at different steps during spliceosome assembly and activation.

Affinity selection of spliceosomal complexes stalled by small-molecule inhibitors of pre-mRNA splicing

For a detailed characterization of the spliceosomal complexes that accumulate in the presence of the novel pre-mRNA splicing inhibitors, we isolated these complexes by size fractionation and affinity chromatography using a MINX pre-mRNA to which three hairpins that bind to the MS2 bacteriophage coat protein had been added (MINX-M3). Splicing reactions were carried out in the presence of inhibitory concentrations of SAHA, splitomicin, DHC, AA, BA3, or garcinol with MINX-M3, which has been pre-bound to a fusion protein of MS2 bacteriophage coat protein and the maltose-binding protein (MS2-MBP). Spliceosomes assembled in the presence of the inhibitors were then separated by glycerol-gradient centrifugation, affinity-selected by binding to amylose beads, and eluted with maltose. Purifications were performed in 150 mM NaCl, in the absence of heparin, to obtain functional splicing complexes (Deckert et al. 2006).

The complexes that assembled in the presence of SAHA, splitomicin, DHC, and BA3 peaked in the 40S region of the glycerol gradient (data not shown), as previously observed for the purification of native spliceosomal B complex (i.e., in the absence of any inhibitor) (Deckert et al. 2006). In contrast, the complexes formed in the presence of AA and garcinol peaked in the region of 25S to 30S (data not shown), as previously observed for the native A complex (Hartmuth et al. 2002; Behzadnia et al. 2006, 2007; Deckert et al. 2006). These results are consistent with those from the native gel analyses described above.

After affinity selection of the six stalled complexes on amylose beads, RNA was in each case recovered from the eluates, separated on a denaturing gel, and visualized by silver staining and autoradiography (Fig. 5). As expected for inhibition before the first catalytic step, mainly unspliced pre-mRNA was present in the purified complexes, with only minor amounts of splicing intermediates (~5% for splitomicin and BA3, 2% for SAHA and DHC, and <1% for AA and garcinol). Small amounts of high-molecular-weight RNA are visible on the gel for all B-type spliceosomes, which most likely represent contamination by

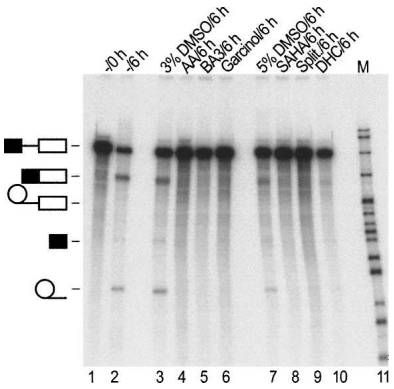

FIGURE 3. Interference by inhibitors of protein acetylation and deacetylation with the splicing of U12-dependent pre-mRNAs. The acetyltransferase inhibitors (lane *4*) AA (0.2 mM), (lane *5*) BA3 (2 mM), and (lane *6*) garcinol (0.2 mM), and the deacetylase inhibitors (lane *8*) SAHA (5 mM), (lane *9*) splitomicin (5 mM), and (lane *10*) DHC (5 mM) were tested for their effect on the splicing in vitro of ^{32}P-labeled U12-dependent p120 pre-mRNA. After the reaction, the radiolabeled RNA was analyzed by denaturing PAGE followed by autoradiography. The positions of pre-mRNA, fully spliced mRNA, lariat-intron/3′-exon, 5′-exon, and lariat-intron (*top* to *bottom*) are indicated on the *left*. (Lane *1*) Input (0 h); (lane *2*) reaction for 6 h without any additive; (lanes *3*,*7*) control reactions with (lane *3*) 3% DMSO and (lane *7*) 5% DMSO.

ribosomal complexes that migrate in the 40S region of the glycerol gradient.

In agreement with the results from the native gel analyses and the migration of the complexes in glycerol gradients, the RNAs of the U1 snRNP, U2 snRNP, and the U4/U6·U5 tri-snRNP were detected in the spliceosomes stalled in the presence of SAHA, splitomicin, DHC, and BA3 (Fig. 5, lanes 1,3,5,9, respectively). However, while U1 snRNA was present in the BA3-stalled complex in similar levels as the other U snRNAs, this snRNA was clearly under-represented in the splicing complexes stalled by SAHA, splitomicin, and DHC (Fig. 5, cf. lane 9 and lanes 1,3,5). This indicates that the U1 snRNP is destabilized by, or dissociates from the spliceosome before, the blockage exerted by SAHA, splitomicin, and DHC; in contrast, the BA3-mediated inhibition of pre-mRNA splicing stalls spliceosome maturation before the release of the U1 snRNP. Thus, spliceosome assembly is apparently blocked by BA3 at a point different from that where the other three inhibitors that still allow B-complex formation exert their effect.

Consistent with the complex formation observed on a native gel, both U1 and U2 snRNAs were found in the AA- and garcinol-stalled complexes, but not the U4, U5, and U6 snRNAs (Fig. 5, lanes 7,11). Thus, even in the absence of heparin, which is added to the splicing reactions analyzed by native gel electrophoresis as shown in Figure 4, no stable incorporation of the U4/U6·U5 tri-snRNP into spliceosomes could be observed, as already suggested by the migration of the complexes in glycerol gradients. This demonstrates clearly that pre-mRNA splicing is blocked in A-like complexes by AA and garcinol. Altogether, the results shown in Figure 5 provide further support for the statement that pre-mRNA splicing is blocked at distinct steps by the novel inhibitors. We refer to the stalled complexes as B^{BA3}, B^{SAHA}, $B^{splitomicin}$, B^{DHC}, A^{AA}, and $A^{garcinol}$.

MS2 affinity-selected stalled splicing complexes are functional intermediates of spliceosome assembly

To investigate whether the MS2 affinity-selected splicing complexes stalled by inhibitors of protein acetylation and deacetylation are functionally committed to splicing, we tried to chase the purified stalled spliceosomes into active splicing complexes. We incubated the affinity-selected A^{AA} and $A^{garcinol}$ spliceosomes under in vitro splicing conditions either with buffer alone, or with nuclear extract that was depleted of the U2 snRNP using a biotinylated antisense-oligonucleotide (ΔU2 nuclear extract). As can be seen by the appearance of fully spliced MINX-M3

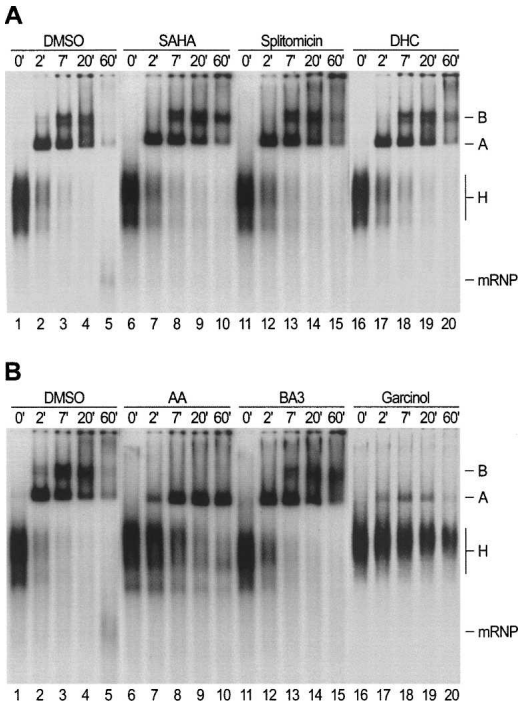

FIGURE 4. Blocking of the pre-mRNA splicing cycle at distinct stages by different inhibitors. (*A*) Formation of splicing complexes on ^{32}P-labeled MINX pre-mRNA in the presence of (lanes *6–10*) 5 mM SAHA, (lanes *11–15*) 2 mM splitomicin, or (lanes *16–20*) 5 mM DHC was monitored on a native agarose gel. Reactions were stopped at the time points indicated in minutes (′) and loaded onto the gel. The positions of the splicing complexes (complex A, complex B, snRNP-free precursor complex H, and the product mRNP) are shown on the *right*. (Lanes *1–5*) Control reaction with the solvent DMSO. (*B*) Formation of splicing complexes on ^{32}P-labeled MINX pre-mRNA in the presence of (lanes *6–10*) 0.2 mM AA, (lanes *11–15*) 2 mM BA3, or (lanes *16–20*) 0.2 mM garcinol was monitored on a native agarose gel as described in *A*. (Lanes *1–5*) Control reaction with DMSO.

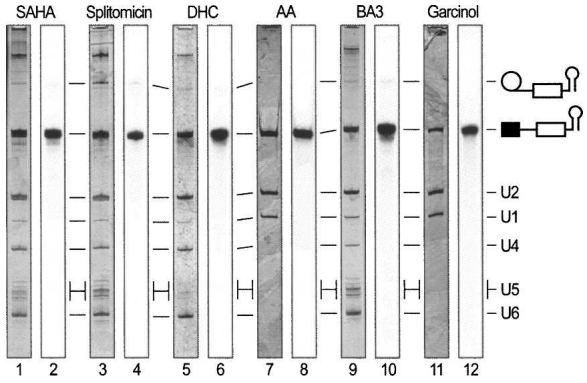

FIGURE 5. RNA composition of HeLa spliceosomal complexes stalled in vitro in the presence of the novel inhibitors of pre-mRNA splicing. Splicing complexes that assemble on MS2-tagged MINX pre-mRNA (MINX-M3) in the presence of SAHA, splitomicin, DHC, AA, BA3, and garcinol were purified by glycerol-gradient centrifugation and affinity selection with amylose beads. RNA was recovered from an aliquot of the purified complexes, separated by denaturing PAGE, and visualized by staining with silver (odd-numbered lanes) and by autoradiography (even-numbered lanes). The positions of lariat-intron/3′-exon, pre-mRNA, and the U snRNAs are indicated on the *right*.

mRNA, purified A^{AA} and $A^{garcinol}$ complexes could be chased into mature spliceosomes that catalyze both transesterification reactions in the presence of ΔU2 nuclear extract, but not with buffer alone (Fig. 6A, lanes 2,3,6,7). To rule out the possibility that the U2 snRNP disassembles from the A complexes during the incubation and then reassembles anew onto the pre-mRNA together with the U1 and U4/U6·U5 snRNPs from the ΔU2 nuclear extract, we performed additional reactions where we added an equimolar amount of naked, untagged MINX pre-mRNA together with the purified A complexes to the mixture. Again, the tagged pre-mRNA present in the A^{AA} and $A^{garcinol}$ complexes underwent splicing (Fig. 6A, lanes 4,8, respectively). In contrast, no splicing of the naked, untagged pre-mRNA can be observed in either case (note that the cleaved 5′ exon and excised lariat-intron generated from both substrates are identical). Thus, spliceosomes are not assembled de novo during the incubation, demonstrating that the A^{AA} and $A^{garcinol}$ complexes are directly converted into active spliceosomes. While only a small portion of the affinity-purified complexes is converted into active spliceosomes, the efficiency of the chase for the A^{AA} and $A^{garcinol}$ complexes is similar to that of an A complex assembled and purified in the absence of any inhibitor (Fig. 6A, lanes 9–12). Altogether, this demonstrates that the A^{AA} and $A^{garcinol}$ spliceosomes are no dead-end complexes, but functional intermediates of the pre-mRNA splicing cycle.

Similarly, we incubated the purified B^{SAHA}, $B^{splitomicin}$, B^{DHC}, and B^{BA3} spliceosomes under in vitro splicing conditions either with buffer alone, or with nuclear extract, in which all endogenous U snRNPs have been degraded by treating with micrococcal nuclease (MN). As shown in Figure 6B, the MS2 affinity-selected B^{SAHA}, $B^{splitomicin}$, B^{DHC}, and B^{BA3} complexes all catalyze the first and second transesterification reaction in the presence of MN-digested nuclear extract (Fig. 6B, lanes 4,12,16,8, respectively). To rule out the possibility that the B complexes dissociate during the incubation and then the released U snRNPs reassemble anew onto the pre-mRNA, we performed splicing reactions with equimolar amounts of purified B complexes and naked, untagged MINX pre-mRNA. As expected, only the tagged pre-mRNA present in the affinity-purified complexes, but not the naked, untagged pre-mRNA, underwent splicing (Fig. 6B, lanes 5,9,13,17; note that the cleaved 5′-exon and excised lariat-intron generated from both substrates are identical), as previously observed with B complex obtained by kinetically controlling the reaction (Deckert et al. 2006). Incubation of the purified B^{SAHA}, B^{BA3}, $B^{splitomicin}$, and B^{DHC} complexes under splicing conditions in the absence of extract did not result in splicing (Fig. 6B, lanes 3,7,11,15, respectively), suggesting that the complexes lack one or more factor(s) required for activation of the spliceosome and/or catalysis of the transesterification reactions. Taken together, these results show that the B complexes stalled upon inhibition of pre-mRNA splicing by SAHA, splitomicin, DHC, or BA3—like the stalled A complexes—are functional spliceosomes and not dead-end complexes.

Protein composition of affinity-selected spliceosomal A^{AA} and $A^{garcinol}$ complexes

To determine the protein composition of the spliceosomal complexes stalled in the presence of the inhibitors, proteins were recovered from affinity-purified spliceosomes and separated by SDS-PAGE. After staining with Coomassie blue, entire lanes were cut into approximately 70 slices; proteins were trypsinized in the gel, extracted, and sequenced by LC-coupled tandem mass spectrometry. According to our previous studies (Deckert et al. 2006; Behzadnia et al. 2007), the number of different sequenced peptides for each identified protein was monitored. Tables 2 and 3 list the identified proteins with their numbers of sequenced peptides in the stalled A and B complexes, respectively. The tables also compare the identified proteins with the proteomes of the native A and B complexes isolated under similar conditions in the absence of any inhibitor (Deckert et al. 2006; Behzadnia et al. 2007). The proteins are grouped according to their reported physical associations, and—for the non-snRNP proteins—their previous identification as belonging to complex A only, or to both A and B complexes, or as being "miscellaneous" proteins.

In agreement with its snRNA composition, the A^{AA} complex was found to contain all proteins of the U1 snRNP and the 17S U2 snRNP, but no U4/U6 or U5

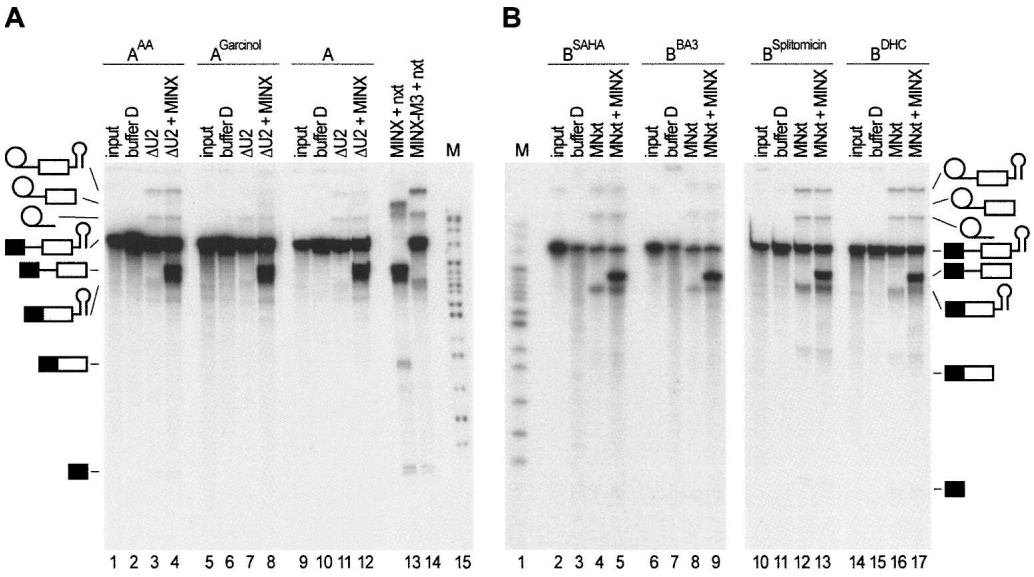

FIGURE 6. MS2 affinity-selected spliceosomal A^{AA}, $A^{garcinol}$, B^{SAHA}, B^{BA3}, $B^{splitomicin}$, and B^{DHC} complexes can be chased into active spliceosomes in appropriately depleted nuclear extract. (*A*) Purified A-type spliceosomal complexes stalled by (lane *1*) AA and (lane *5*) garcinol (input) were incubated under splicing conditions in the presence of (lanes *2*,*6*) buffer D, (lanes *3*,*7*) nuclear extract depleted of the 12S U2 snRNP (ΔU2), or (lanes *4*,*8*) together with an equimolar amount of naked, untagged MINX pre-mRNA in the presence of ΔU2 nuclear extract (ΔU2+MINX). (Lanes *9*–*12*) As a control for the efficiency of the chase, the same set of reactions was also performed with a "wild-type" A complex (A) assembled and purified in the absence of any inhibitor. Furthermore, one standard splicing reaction each with (lane *13*) naked, untagged MINX pre-mRNA and (lane *14*) naked, tagged MINX-M3 pre-mRNA using nuclear extract (nxt) was performed. After the reaction, the radiolabeled RNA was analyzed by denaturing PAGE followed by autoradiography. The positions of lariat-intron/3′-exon (MINX-M3), lariat-intron/3′-exon (MINX), lariat-intron (MINX-M3), pre-mRNA (MINX-M3), pre-mRNA (MINX), fully spliced mRNA (MINX-M3), fully spliced mRNA (MINX), and 5′-exon (MINX-M3) (from *top* to *bottom*) are indicated schematically on the *left*. (Lane *15*) Size marker (M). (*B*) Purified B-type spliceosomal complexes stalled by (lane *2*) SAHA, (lane *6*) BA3, (lane *10*) splitomicin, and (lane *14*) DHC (input) were incubated under splicing conditions in the presence of (lanes *3*,*7*,*11*,*15*) buffer D, (lanes *4*,*8*,*12*,*16*) micrococcal nuclease (MN)-treated nuclear extract (MNxt), or (lanes *5*,*9*,*13*,*17*) together with an equimolar amount of naked, untagged MINX pre-mRNA in the presence of MN-treated nuclear extract (MNxt+MINX). After the reaction, the radiolabeled RNA was analyzed by denaturing PAGE followed by autoradiography. The positions of the individual RNAs are indicated schematically on the *right* as in *A*. (Lane *1*) Size marker (M).

proteins (Table 2). The most obvious differences in the protein composition between the A^{AA} complex and native A complexes are the lack of the U1 snRNP-associated proteins FBP11 and S164 (fSAP94). Furthermore, no 17S U2-related protein DExD/H-box helicase hPRP5 could be detected in A^{AA} complex. Interestingly, we also observed that SR and SR-related proteins were clearly under-represented (in terms of numbers of sequenced peptides) or are completely absent. Besides two peptides for CCAP1 (also called hsp73), no evidence for proteins of the hPRP19/CDC5 complex, which was recently shown to be associated with the native A complex (Behzadnia et al. 2007), was found in the stalled A^{AA} complex. Similarly, almost all non-snRNP proteins previously detected only in the A or in both A and B complexes (e.g., SF1 and p68) were absent as well. However, interesting exceptions are the proteins NFAR and NF45, which form a heterodimer and have been implicated in mRNA processing (Isken et al. 2003; Merz et al. 2007). These were prominent in the A^{AA} complex, with 75 and 21 peptides, respectively, while they were apparently only marginally present in the native A complexes isolated by Behzadnia et al. (2007). We also detected nucleolin by a surprisingly high number of sequenced peptides (more than 100) in A^{AA} complex among seven novel proteins that had not been reported to be associated with pre-mRNA splicing yet.

The set of proteins found in the $A^{garcinol}$ complex is more restricted than in the A^{AA} complex. The U1 snRNP proteins were clearly under-represented, and the U1-related proteins were completely missing, indicating that U1 snRNP is more loosely associated with this stalled complex. Most U2 and U2-related proteins could be identified, with the exception of hPrp5 and SPF31, which were again absent, similarly to the situation in A^{AA} complexes. Interestingly, significantly more peptides derived from hPrp43 and SR140 (fSAPa) were sequenced in the $A^{garcinol}$ than in the A^{AA} complexes, indicating that both these proteins are more abundant in $A^{garcinol}$ complexes. While in the A^{AA} complex a limited number of SR proteins could still be detected, these are completely absent in $A^{garcinol}$. Moreover, all other proteins—including hnRNPs, Prp19/CDC5 and related proteins, and proteins that were previously detected only in A or in both A and B complexes—were either completely absent or detectable with only a very small number of sequenced

TABLE 2. Protein composition of spliceosomal A complexes stalled in the presence of inhibitors

Protein	Mol mass (kDa)	GenBank accession number	Number of peptides sequenced in A complex preparation			Gene	
			A (2.1 pmol)	A^{AA} (5.5 pmol)	$A^{garcinol}$ (3.9 pmol)	*Saccharomyces cerevisiae*	*Schizosaccharomyces pombe*
Sm proteins							
B	24.6	gi|4507125	20	43	8	*SMB1*	*smb1*
D1	13.3	gi|5902102	7	30	2	*SMD1*	*smd1*
D2	13.5	gi|29294624	32	68	14	*SMD2*	*smd2*
D3	13.9	gi|4759160	24	15	8	*SMD3*	*smd3*
E	10.8	gi|4507129	25	11	7	*SME1*	*sme1*
F	9.7	gi|4507131	7	6	2	*SMX3*	*smf1*
G	8.5	gi|4507133	15	6	2	*SMX2*	*smg1*
U1 snRNP							
U1-70K	51.6	gi|29568103	67	49	1 (21)	*SNP1*	*usp101*
U1-A	31.3	gi|4759156	38	27	3	*MUD1*	*usp102*
U1-C	17.4	gi|4507127	2	7		*YHC1*	*usp103*
U1 snRNP-related							
FBP11	48.5	gi|88953744	18			*PRP40*	*usp104*
S164 (fSAP94)	100.1	gi|4050087	13			*SNU71*	*usp107*
17S U2 snRNP							
U2A′	28.4	gi|50593002	32	49	14	*LEA1*	*SPBC1861.08c*
U2B″	25.4	gi|4507123	16	16	10	*MSL1*	*SPBC8D2.09c*
SF3a120	88.9	gi|5032087	90	63	59	*PRP21*	*sap114*
SF3a66	49.3	gi|21361376	7	17	6	*PRP11*	*sap62*
SF3a60	58.5	gi|5803167	21	45	21	*PRP9*	*sap61*
SF3b155	145.8	gi|54112117	77	130	62	*HSH155*	*prp10*
SF3b145	100.2	gi|55749531	53	131	124	*CUS1*	*sap145*
SF3b130	135.5	gi|54112121	196	171	140	*RSE1*	*prp12*
SF3b49	44.4	gi|5032069	8	2	6	*HSH49*	*sap49*
SF3b14a/p14	14.6	gi|7706326	15	21	9		*SPBC29A3.07c*
SF3b14b	12.4	gi|14249398	12	15	5	*RDS3*	*ini1*
SF3b10	10.1	gi|13775200	2	7		*YSF3*	*SPBC211.05*
17S U2-related							
hPRP43	90.9	gi|68509926	37	12	52	*PRP43*	*prp43*
SPF45	45.0	gi|14249678	9		7		
SPF30	26.7	gi|5032113	10	13	4		*spf30*
U2AF65	53.5	gi|6005926	8	7	3	*MUD2*	*prp2*
U2AF35	27.9	gi|5803207	5	3	4		*SPAP8A3.06*
SPF31	31.0	gi|7657611	8				*spf31*
hPRP5	117.4	gi|41327773	10			*PRP5*	*prp11*
SR140 (fSAPa)	118.2	gi|51492636	3		25		*SPBC11C11.01*
CHERP	100.0	gi|21359884	2		5		
PUF60	59.9	gi|17298690	10	5	1 (27)		
SR proteins							
SF2/ASF	27.8	gi|5902076	69	28	2		
9G8	27.4	gi|72534660	29	19	6		
SRp20	19.4	gi|4506901	10	2			
SRp30c	25.5	gi|4506903	30	17			
SRp40	31.3	gi|3929378	25				
SRp55	39.6	gi|20127499	29				
SRp75	56.8	gi|21361282	7				
SC35	25.5	gi|47271443	8				
SR-related proteins							
FLJ10154	32.9	gi|48675817	6				
SRm160	102.5	gi|3005587					*SPCC825.05c*
SRm300	300.0	gi|19923466	1			*CWC21 (?)*	*cwf21 (?)*
hnRNPs							
hnRNP A0	30.9	gi|5803036			1 (58)		

(*continued*)

TABLE 2. *Continued*

Protein	Mol mass (kDa)	GenBank accession number	Number of peptides sequenced in A complex preparation			Gene	
			A (2.1 pmol)	A^{AA} (5.5 pmol)	$A^{garcinol}$ (3.9 pmol)	*Saccharomyces cerevisiae*	*Schizosaccharomyces pombe*
hnRNP A1	38.7	gi|4504445	43	36			
hnRNP A3	39.6	gi|34740329	4	6			
hnRNP AB	36.0	gi|12803583	2	6			
hnRNP A2/B1	37.4	gi|14043072	17	1 (20)			
hnRNP C1/C2	33.3	gi|4758544	24	7	11		
hnRNP D	38.4	gi|14110420		12			
hnRNP L	64.1	gi|52632383		2			
hnRNP Q	69.6	gi|23397427	2	18			
hnRNP R	70.9	gi|5031755		7			
hnRNP U	90.6	gi|14141161	3				
hnRNP U-like 1 (E1B-AP5)	95.7	gi|21536326		32			
hnRNP U-like 2	72.4	gi|52545896		3			
PCBP1	37.5	gi|5453854	8			*HEK2 (?)*	*rnc1 (?)*
Cap binding complex							
CBP20	18.0	gi|19923387	9	25		*CBC2*	*SPBC13A2.01c*
CBP80	91.8	gi|4505343	9	43	24	*STO1*	*SPAC6G10.07*
hPRP19/CDC5 complex							
hPRP19	55.2	gi|7657381	7			*PRP19*	*prp19*
CDC5 (CDC5L)	92.2	gi|11067747	6			*CEF1*	*cdc5*
SPF27	21.5	gi|5031653	3			*SNT309*	*cwf7*
CCAP1 (hsp73)	70.4	gi|5729877	3	2		*SSA1*	*ssa1*
CCAP2 (hspc148, AD-002)	26.6	gi|7705475	9			*CWC15*	*cwf15*
Catenin β-like 1	65.1	gi|18644734	5				*SPAC1952.06c*
Npw38BP	70.0	gi|7706501	5				
Npw38	30.5	gi|5031957	1				
PRCC	52.4	gi|40807447	2				
Non-snRNP proteins (previously detected in A complex)							
Acinus (fSAP152)	151.8	gi|7662238	4				
BUB3	37.2	gi|4757880	16			*BUB3*	*bub3*
CDK11 (CDC2L2)	91.0	gi|16357494	1				*ppk23*
FLJ10839	132.8	gi|46852388	7	4	3		
MGC2803 (fSAP18)	18.4	gi|13128992	10				
Pinin	81.6	gi|33356174					
RBM10	103.5	gi|12644371	8	2	9		*SPAC17H9.04c (?)*
RBM5/LUCA15	92.1	gi|5032031	4				
RNPS1	34.2	gi|6857826	1				*SPBC13G1.14c*
SF1	68.3	gi|42544130	7			*MSL5*	*bpb1*
SF4 (F23858)	72.5	gi|33469964	13	2		*YNL224C (?)*	*SPAC2G11.04 (?)*
tat SF1	85.7	gi|21361437	4			*CUS2*	*uap2*
ZNF207	50.8	gi|4508017	4				
Non-snRNP proteins (previously detected in A and B complexes)							
NFAR	95.4	gi|24234750	8	75	63		
NF45	43.0	gi|24234747		21	28		
ASR2B	100.0	gi|58331218	56	3	2		*SPBC725.08*
DDX9	142	gi|4503297	1	1 (28)	7		
ELAV (HuR)	36.1	gi|38201714	3		1 (27)		
HCNGP	33.9	gi|9994179					*SPAC3H1.03*
hsp27	22.8	gi|4504517		1 (38)			
LOC124245	104.0	gi|31377595	9				
NRIP2	31.3	gi|13899327	6				
p68 (DDX5)	69.2	gi|4758138	21			*(DBP2)*	*(dbp2)*
p72/DDX17	80.5	gi|3122595	2	4		*(DBP2)*	*(dbp2)*

(*continued*)

TABLE 2. *Continued*

Protein	Mol mass (kDa)	GenBank accession number	Number of peptides sequenced in A complex preparation			Gene	
			A (2.1 pmol)	A^{AA} (5.5 pmol)	$A^{garcinol}$ (3.9 pmol)	*Saccharomyces cerevisiae*	*Schizosaccharomyces pombe*
RNPC2 (CAPER, fSAP59)	59.4	gi|4757926	15				*rsd1*
TCERG1 (CA150)	123.9	gi|21327715	11			*YPR152C*	*dre4*
YB-1	35.9	gi|34098946	2				
Miscellaneous							
Nucleolin	76.5	gi|55956788		103	2	*NSR1*	*gar2*
DHX36	114.8	gi|18497286		11		*YLR419W (?)*	*ucp12 (?)*
eEF1A2	50.5	gi|4503475		5	2	*TEF2*	*ef1a-c*
eIF2AK2 (PRKR)	62.1	gi|4506103		4			
LSm14A	50.5	gi|24308093		1 (47)		*SCD6*	*sum2*
RDBP	43.2	gi|14670268		2			
ZC3HAV1	101.4	gi|27477136		9			

Splicing complexes were stalled in the presence of the inhibitors as indicated, and the proteins present in these complexes were identified by mass spectrometry after separation by SDS-PAGE (the amount loaded on the gel is listed in parentheses). The presence of a protein in the individual complex preparations is indicated by a number, which represents the absolute number of peptides sequenced for that protein. Note that several proteins were detected in multiple bands. If only one peptide has been identified for a given protein in a preparation, the score for this peptide is given in parentheses. Proteins previously identified in the double affinity-purified A complex assembled in the absence of any inhibitor (Behzadnia et al. 2007) are indicated with the numbers of peptides sequenced for each protein as explained above. Calculated molecular masses and accession numbers in the GenBank database at the NCBI are indicated. The gene names of the *S. cerevisiae* and *S. pombe* homologs of the indicated human protein are given. A question mark indicates that it is currently not clear whether the indicated yeast protein is a true functional homolog. BLAST alignments of both p68 (DDX5) and p72 (DDX17) revealed significant homology with *S. cerevisiae DBP2* and *S. pombe dbp2* (between 56% and 59% sequence identity, respectively). Since true homology remains to be verified, *DBP2* and *dbp2* are both enclosed in parentheses.

peptides. Interestingly, NFAR and NF45 proteins were again detected by an increased number of sequenced peptides. In contrast, only two peptides of nucleolin were detected in the $A^{garcinol}$ complex, while more than 100 peptides of this protein were found in the A^{AA} complex.

Protein composition of affinity-selected stalled spliceosomal B complexes

As described above for the A^{AA} and $A^{garcinol}$ complexes, we determined the protein composition of the B^{BA3}, B^{SAHA}, $B^{splitomicin}$, and B^{DHC} complexes. In accordance with the RNA analysis and in agreement with the protein content of a B complex assembled and purified in the absence of any inhibitor (Deckert et al. 2006), the B-type spliceosomes stalled by BA3, SAHA, splitomicin, or DHC contained all the proteins of the 17S U2 and the U4/U6·U5 snRNPs (Table 3), but they varied with respect to the presence of the U1 snRNP proteins. The fact that the peptide numbers for certain proteins of the U snRNPs (e.g., SmD2, SmG, SF3b130; U5 116K, U4/U6 90K, and 61K, U4/U6·U5 110K) varied among the B complex samples made it difficult to define precise effects of the inhibitors on the amounts of individual proteins in the corresponding complexes. Nonetheless, a few noteworthy changes at the protein level could be observed for each group of proteins:

1. In B^{SAHA}, B^{DHC}, and $B^{splitomicin}$, the U1 proteins were under-represented or completely absent, whereas in B^{BA3} the number of sequenced peptides from U1 70K was significantly higher, suggesting an opposite effect, i.e., more U1 snRNP is associated with these complexes.
2. Only in the B^{BA3} complex were we able to sequence peptides for the U1 snRNP-related proteins FBP11 and S164; this may be related to the higher amount of U1 (U1 70K) present in the sample.
3. The association of 17S U2 proteins and 17S U2-related proteins with B complexes does not seem to be affected drastically upon treatment with inhibitors. Exceptions are the 17S U2-related proteins hPrp43 and SPF45 in B^{BA3} complexes which, in terms of numbers of sequenced peptides, seem to be more abundant than the other complexes.
4. All the U5, U4/U6, and U4/U6·U5 proteins were identified unambiguously. Still, some protein abundances seem to be affected, i.e., protein TFIP11 in B^{BA3} was identified by significantly more peptides than in the other complexes.
5. The number of peptides derived from the SR proteins is reduced in the stalled B complexes. In particular, SF2/ASF in B^{SAHA} and 9G8 in all stalled B complexes seem to be less abundant than in the native B complex. In contrast, the SR-related SRm300 protein, which was

TABLE 3. Protein composition of spliceosomal B complexes stalled in the presence of inhibitors

Protein	Mol mass (kDa)	GenBank accession number	Number of peptides sequenced in B complex preparation						Gene	
			$B^{\#1}$ (4.4 pmol)	$B^{\#2}$ (5.1 pmol)	B^{BA3} (8.8 pmol)	B^{SAHA} (5.0 pmol)	B^{DHC} (4.1 pmol)	$B^{Split.}$ (4.1 pmol)	*Saccharomyces cerevisiae*	*Schizosaccharomyces pombe*
Sm proteins										
B	24.6	gi|4507125	84	74	35	33	79	58	*SMB1*	*smb1*
D1	13.3	gi|5902102	18	48	11	6	20	22	*SMD1*	*smd1*
D2	13.5	gi|29294624	32	103	50	35	71	51	*SMD2*	*smd2*
D3	13.9	gi|4759160	65	45	41	25	37	29	*SMD3*	*smd3*
E	10.8	gi|4507129	45	28	11	45	23	20	*SME1*	*sme1*
F	9.7	gi|4507131	11	5	23	17	35	34	*SMX3*	*smf1*
G	8.5	gi|4507133	28	11	5	32	7	2	*SMX2*	*smg1*
U1 snRNP										
U1-70K	51.6	gi|29568103	10	14	51	6	2		*SNP1*	*usp101*
U1-A	31.3	gi|4759156	12	27	28	15	3	1 (19)	*MUD1*	*usp102*
U1-C	17.4	gi|4507127	1 (24)	2		4	1 (79)	2	*YHC1*	*usp103*
U1 snRNP-related										
FBP11	48.5	gi|88953744			3				*PRP40*	*usp104*
S164 (fSAP94)	100.1	gi|4050087			3				*SNU71*	*usp107*
17S U2 snRNP										
U2A′	28.4	gi|50593002	41	67	73	121	115	96	*LEA1*	*SPBC1861.08c*
U2B″	25.4	gi|4507123	31	28	18	43	29	29	*MSL1*	*SPBC8D2.09c*
SF3a120	88.9	gi|5032087	71	43	86	64	144	147	*PRP21*	*sap114*
SF3a66	49.3	gi|21361376	24	56	20	46	26	27	*PRP11*	*sap62*
SF3a60	58.5	gi|5803167	52	7	78	50	92	59	*PRP9*	*sap61*
SF3b155	145.8	gi|54112117	111	109	239	187	259	232	*HSH155*	*prp10*
SF3b145	100.2	gi|55749531	70	69	116	67	193	158	*CUS1*	*sap145*
SF3b130	135.5	gi|54112121	252	93	227	132	501	369	*RSE1*	*prp12*
SF3b49	44.4	gi|5032069	9	10	7	9	5	9	*HSH49*	*sap49*
SF3b14a/p14	14.6	gi|7706326	20	30	20	26	37	39		*SPBC29A3.07c*
SF3b14b	12.4	gi|14249398	12	12	18	18	13	22	*RDS3*	*ini1*
SF3b10	10.1	gi|13775200	6	2	3	2	7	7	*YSF3*	*SPBC211.05*
17S U2 snRNP-related										
hPRP43	90.9	gi|68509926	29	28	45	29	14	12	*PRP43*	*prp43*
SPF45	45.0	gi|14249678	2	5	18	4	5	6		
SPF30	26.7	gi|5032113	8	18	7	20	19	15		*spf30*
U2AF65	53.5	gi|6005926	18	11	6	6	16	8	*MUD2*	*prp2*
U2AF35	27.9	gi|5803207	7	26	9	4	14	8		*SPAP8A3.06*
SPF31	31.0	gi|7657611			5					*spf31*
SR140 (fSAPa)	118.2	gi|51492636		8	4	4		3		*SPBC11C11.01*
CHERP	100.0	gi|21359884		3		2				
U5 snRNP										
220K	273.7	gi|3661610	184	306	286	204	590	549	*PRP8*	*spp42*
200K	244.5	gi|45861372	95	267	273	158	605	488	*BRR2*	*brr2*
116K	109.4	gi|41152056	153	76	205	90	397	351	*SNU114*	*cwf10*
40K	39.3	gi|4758560	28	34	31	32	44	53	*LIN1*	*SPBC83.09c*
102K	106.9	gi|40807485	78	99	113	72	253	155	*PRP6*	*prp1*

(*continued*)

TABLE 3. *Continued*

Protein	Mol mass (kDa)	GenBank accession number	Number of peptides sequenced in B complex preparation						Gene	
			$B^{\#1}$ (4.4 pmol)	$B^{\#2}$ (5.1 pmol)	B^{BA3} (8.8 pmol)	B^{SAHA} (5.0 pmol)	B^{DHC} (4.1 pmol)	$B^{Split.}$ (4.1 pmol)	*Saccharomyces cerevisiae*	*Schizosaccharomyces pombe*
100K	95.6	gi|41327771	33	48	40	11	27	13	*PRP28*	*prp28*
15K	16.8	gi|5729802	5	7	6	16	18	7	*DIB1*	*dim1*
LSm proteins										
LSm2	10.8	gi|10863977	17	14	8	22	25	12	*LSM2*	*lsm2*
LSm3	11.8	gi|7657315	3	5	6	2	5	7	*LSM3*	*lsm3*
LSm4	15.4	gi|6912486	23	21	16	12	21	14	*LSM4*	*lsm4*
LSm5	9.9	gi|6912488							*LSM5*	*lsm5*
LSm6	9.1	gi|5919153	8	20		24			*LSM6*	*lsm6*
LSm7	11.6	gi|7706423	6	4	6	3	9	7	*LSM7*	*lsm7*
LSm8	10.4	gi|7706425	1 (58)	7	2	4	4	3	*LSM8*	*lsm8*
U4/U6 snRNP										
90K	77.6	gi|4758556	82	85	61	131	109	77	*PRP3*	*prp3*
60K	58.4	gi|45861374	49	41	35	52	117	78	*PRP4*	*SPAC227.12*
20K	20.0	gi|5454154	22	46	22	31	50	43	*CPR3*	*cyp3*
61K	55.4	gi|40254869	62	53	40	100	61	46	*PRP31*	*prp31*
15.5K	14.2	gi|4826860	2	8	8	12	14	11	*SNU13*	*snu13*
U4/U6.U5 snRNP										
110K	90.2	gi|13926068	29	64	60	58	128	114	*SNU66*	*snu66*
65K	65.4	gi|56550051	15	35	15	10	20	11	*SAD1*	*ubp10*
27K	18.9	gi|24307919								*SPCC162.01c*
hSnu23	23.6	gi|21389511	3	4	11	14	8	11	*SNU23*	*snu23*
hPrp38	37.5	gi|24762236	11	24	29	16	26	28	*PRP38*	*prp38*
TFIP11	96.8	gi|8393259	1 (44)	14	39	1 (22)	3	5	*SPP382*	*SPAC1486.03c*
SR proteins										
SF2/ASF	27.8	gi|5902076	18	37	25	3	15	16		
9G8	27.4	gi|72534660	13	22	4	3		5		
SRp20	19.4	gi|4506901				1 (22)		1 (17)		
SRp30c	25.5	gi|4506903	4		8	5	5	5		
SRp38	31.3	gi|5730079	2		1 (42)		1			
SRp40	31.3	gi|3929378	9	4		3				
SRp55	39.6	gi|20127499	6	2	1 (33)					
SRp75	56.8	gi|21361282		2		1 (12)				
SR-related proteins										
FLJ10154	32.9	gi|48675817	2		4					
SRm160	102.5	gi|3005587		4		3				*SPCC825.05c*
SRm300	300.0	gi|19923466					10	12	*CWC21 (?)*	*cwf21 (?)*
hnRNPs										
hnRNP A0	30.9	gi|5803036	16	10	7	14	5	2		
hnRNP A1	38.7	gi|4504445	38	27	16	15	11	13		
hnRNP A3	39.6	gi|34740329	4	2		4	3	1 (49)		
hnRNP A2/B1	37.4	gi|14043072	9	4		1 (23)		2		
hnRNP C1/C2	33.3	gi|4758544	11	5	21	2	2	2		

(*continued*)

TABLE 3. *Continued*

Protein	Mol mass (kDa)	GenBank accession number	Number of peptides sequenced in B complex preparation						Gene	
			$B^{\#1}$ (4.4 pmol)	$B^{\#2}$ (5.1 pmol)	B^{BA3} (8.8 pmol)	B^{SAHA} (5.0 pmol)	B^{DHC} (4.1 pmol)	$B^{Split.}$ (4.1 pmol)	*Saccharomyces cerevisiae*	*Schizosaccharomyces pombe*
hnRNP F	45.7	gi|4826760		3						
hnRNP G	42.4	gi|56699409		8	16	4				
hnRNP H2	49.3	gi|9624998	1 (81)				1 (70)	2		
hnRNP M	77.5	gi|14141152		12	14	3	3	3		
hnRNP Q	69.6	gi|23397427	4			1 (33)				
hnRNP U-like 1 (E1B-AP5)	95.7	gi|21536326			16		2	3		
PCBP1	37.5	gi|5453854	7	14	9	2	4	3	*(HEK2 [?])*	*(rnc1 [?])*
PCBP2	38.6	gi|14141168			4				*(HEK2 [?])*	*(rnc1 [?])*
RALY	32.5	gi|8051631	2		7	3				
Cap binding complex										
CBP20	18.0	gi|19923387	4	16	23	15	20	28	*CBC2*	*SPBC13A2.01c*
CBP80	91.8	gi|4505343	2	45	50	51	48	41	*STO1*	*SPAC6G10.07*
hPRP19/CDC5 complex										
hPRP19	55.2	gi|7657381	46	50	85	56	92	139	*PRP19*	*prp19*
CDC5 (CDC5L)	92.2	gi|11067747	43	50	68	49	93	110	*CEF1*	*cdc5*
SPF27	21.5	gi|5031653	21	20	29	25	18	30	*SNT309*	*cwf7*
PRL1 (PRLG1)	57.2	gi|4505895	19	20	18	21	30	45	*PRP46*	*prp5*
CCAP1 (hsp73)	70.4	gi|5729877		5	13	8	2	6	*SSA1*	*ssa1*
CCAP2 (hspc148, AD-002)	26.6	gi|7705475	7	13	12	10	18	39	*CWC15*	*cwf15*
Catenin β-like 1	65.1	gi|18644734	9	11	2	6	8	10		*SPAC1952.06c*
Npw38BP	70.0	gi|7706501	25	42	86	22	48	46		
Npw38	30.5	gi|5031957	19	17	26	16	19	25		
hPRP19/CDC5-related										
PRCC	52.4	gi|40807447	1 (22)	4		4	10	9		
hECM2 (fSAP47)	46.9	gi|8922328	8	1 (39)	13	6	65	85	*ECM2*	*cwf5*
hSYF1 (XAB2)	100.0	gi|55770906	15	45	48	39	47	84	*SYF1*	*cwf3*
CRNKL1/hSYF3	100.6	gi|30795220	16	44	44	43	44	52	*CLF1*	*cwf4*
hIsy1 (fSAP133)	33.0	gi|20149304	3	12	12	6	13	28	*ISY1*	*cwf12*
SKIP	51.1	gi|6912676	28	41	66	48	83	108	*PRP45*	*prp45*
Cyp-E	33.4	gi|5174637	8	11	26	12	11	23		
PPIase-like 1 (PPIL1)	18.2	gi|7706339	8	14	16	13	23	44		
KIAA0560 (fSAP164)	171.3	gi|38788372		39	41	37	37	82		*cwf11*
G10 (fSAP17)	17.0	gi|32171175	8	20	21	8	31	34	*BUD31*	*cwf14*
RES complex										
SNIP1	45.8	gi|21314720	5	3	8	14	9	22	*PML1*	
MGC13125 (fSAP71)	70.5	gi|14249338	6	13	9	4	6	9	*BUD13*	*cwf26*
CGI-79	39.7	gi|4929627	1 (33)	1 (32)	5			2	*IST3*	*cwf29*
Non-snRNP proteins (previously detected in A complex)										
Acinus (fSAP152)	151.8	gi|7662238				1 (48)				
BUB3	37.2	gi|4757880				3			*BUB3*	*bub3*
CDK11 (CDC2L2)	91.0	gi|16357494			19					*ppk23*
FLJ10839	132.8	gi|46852388						4		
KRIT1	84.4	gi|37221187			1 (30)					

(*continued*)

TABLE 3. *Continued*

Protein	Mol mass (kDa)	GenBank accession number	Number of peptides sequenced in B complex preparation						Gene	
			$B^{\#1}$ (4.4 pmol)	$B^{\#2}$ (5.1 pmol)	B^{BA3} (8.8 pmol)	B^{SAHA} (5.0 pmol)	B^{DHC} (4.1 pmol)	$B^{Split.}$ (4.1 pmol)	*Saccharomyces cerevisiae*	*Schizosaccharomyces pombe*
MGC2803 (fSAP18)	18.4	gi|13128992				1 (32)				
SF4 (F23858)	72.5	gi|33469964			3				*YNL224C (?)*	*SPAC2G11.04 (?)*
Non-snRNP proteins (previously detected in A and B complexes)										
ASR2B	100.0	gi|58331218	8	47	25	3	2	4		*SPBC725.08*
eEF1A2	50.5	gi|4503475			3	4			*TEF2*	*ef1a-c*
ELAV (HuR)	36.1	gi|38201714	3	10	3	4				
HCNGP	33.9	gi|9994179			11					*SPAC3H1.03*
LOC124245 (hNHN1)	104.0	gi|31377595	5	53	19			4		
NF45	43.0	gi|24234747	13	6	6	1 (21)		1 (25)		
NRIP2	31.3	gi|13899327	9		2	2				
p68 (DDX5)	69.2	gi|4758138		5	10		4	10	*(DBP2)*	*(dbp2)*
RBM10	103.5	gi|12644371	2		2	1 (17)				*SPAC17H9.04c (?)*
RNPC2 (CAPER, fSAP59)	59.4	gi|4757926	46	33	11	15	13	4		*rsd1*
TCERG1 (CA150)	123.9	gi|21327715	3	14	20	5	3	19	*URN1*	*dre4*
YB-1	35.9	gi|34098946	17	25	10	22	4	10		
Non-snRNP proteins (previously detected in B complex)										
Abstrakt	69.8	gi|21071032		2	3	4	1 (27)	5		
FBP21	42.5	gi|6005948	4	8	8	11	11	7		*SPBC18H10.07*
GCIP p29 (fSAP29)	28.7	gi|7661636		5	20	1 (55)	3	10	*SYF2*	*SPBC3E7.13c*
hPRP2	119.2	gi|4503293	3	8	10	33	15	33	*PRP2*	*cdc28*
hPRP4-Kinase	117.1	gi|17999535		1 (34)			2			*prp4*
HsKin17	45.4	gi|13124883		11	13	9	10	10	*RTS2*	*SPBC365.09c*
hSmu-1 (fSAP57)	57.5	gi|8922679	26	40	160	47	89	74		
hsp27	22.8	gi|4504517	2	4	4	2	6	3		
KIAA0073 (CyP64, PPWD1)	73.6	gi|24308049		4	2	4	2	2		
KIAA1604 (fSAPb)	105.5	gi|55749769		6	10	5	3	24	*CWC22*	*cwf22*
LOC51325 (fSAP105)	104.8	gi|22035565		11	18	1 (61)	11	2		
LOC84081/DKFZp434k1421	66.4	gi|14149807	1 (22)	5	7	8	5	11		*SPAC29A4.06c*
Matrin 3	94.6	gi|21626466		4	5				*ECM13*	
MFAP1	51.9	gi|50726968	23	23	57	36	51	59		*SPAC1782.03*
MGC20398	42.0	gi|49472814	3		2	4	3	8		
MGC23918	19.2	gi|21389497	4	6	8	16	12	33		*cwf18*
NY-CO-10	53.8	gi|64276486		6	2	5	5	10	*CWC27*	*cyp7*
PABP	70.7	gi|46367787	4					1 (34)	*PAB1*	*SPAC57A7.04c*
PPIL2/Cyp-60	59.5	gi|7657473	1 (16)	27	2	10	9	25		
PPIL4	57.2	gi|20911035	1 (15)	3	6	5	4	14		
RBM7	30.5	gi|5070698	2	6	4		3			
RED	65.6	gi|10835234	31	35	112	39	92	103		*SPBC1539.02*
UBL5	8.5	gi|13236510	6	7	11	2	16	24	*HUB1*	*hub1*
Non-snRNP proteins (step II/mRNP proteins)										
Aly/REF	26.9	gi|55770864			5				*YRA1*	*mlo3*
eIF4A3	46.9	gi|7661920			23	9	5	11	*FAL1 (?)*	*SPAC1F5.10*
ELG	38.9	gi|8923771			11					*SPCC16C4.16c (?)*

(*continued*)

TABLE 3. *Continued*

Protein	Mol mass (kDa)	GenBank accession number	Number of peptides sequenced in B complex preparation						Gene	
			$B^{\#1}$ (4.4 pmol)	$B^{\#2}$ (5.1 pmol)	B^{BA3} (8.8 pmol)	B^{SAHA} (5.0 pmol)	B^{DHC} (4.1 pmol)	$B^{Split.}$ (4.1 pmol)	*Saccharomyces cerevisiae*	*Schizosaccharomyces pombe*
hPRP16	140.5	gi|17999539					1 (21)		*PRP16*	*prp16*
hPRP17	65.5	gi|7706657	1 (36)	8	22	26	11	11	*CDC40*	*prp17*
hPRP22	139.3	gi|4826690			5	4		6	*PRP22*	*prp22*
hSLU7	68.4	gi|27477111		1 (39)	2	4	1 (30)	6	*SLU7*	*slu7*
Magoh	17.2	gi|4505087		1 (56)				1 (50)		*SPBC3B9.08c*
THOC3	38.8	gi|14150171					1 (26)		*TEX1*	*SPCC18B5.10c*
UAP56	49.1	gi|21040371		3	1 (30)				*SUB2*	*uap56*
Y14	19.9	gi|4826972				2	3	2		*SPAC23A1.09*
Miscellaneous										
BRPF3	135.8	gi|55742815			3					
C9orf78 (LOC51759)	33.7	gi|7706557				1 (32)		3		
CCDC18	163.9	gi|62243484				3				
DBPA	40.1	gi|14602477			8	5				
DDX35	78.9	gi|20544129			10	2		2		
FLJ20291	49.7	gi|8923271			1 (29)	5	3	1 (51)	*CWC25*	*cwf25*
FLJ22965	25.6	gi|11545813			3	3	1 (50)	3		
FRG1	29.2	gi|4758404			2	6	4	15		*SPBP23A10.12*
GPATC1 (Q9BRR8)	103.3	gi|21361684			4	1 (42)				*SPAC20H4.06c*
GPKOW (GPATC5)	52.2	gi|15811782						1 (26)	*SPP2*	*cwf28*
GTL3 (fSAP23)	22.8	gi|8392875						2		
IQGAP1	189.2	gi|4506787			2					
KIAA0100	253.7	gi|57242774					6	9		
MORG1	34.3	gi|14150114			6					
NOSIP	33.2	gi|7705716			3					
PPIase-like 3b	18.6	gi|14277126						2		
PRKRIP1	21.0	gi|13375901			2	5	1 (41)	2		
RACK1 (GNB2L1)	35.1	gi|5174447					3	3	*ASC1*	*cpc2*
RNF113A	38.8	gi|5902158						7	*CWC24*	*cwf24*
RSRC1	38.7	gi|38488727			5					
SEC31-like 2	128.7	gi|14149696			10	7	4	9	*SEC31*	*sec31*
SKIV2L2 (fSAP118)	117.8	gi|39930353			1 (51)				*MTR4*	*SPAC6F12.16c*
WDR70	73.2	gi|8922301			6		6	9		
ZC3HAV1	101.4	gi|27477136				3	1 (76)	1 (58)		

Splicing complexes were stalled in the presence of the inhibitors as indicated, and the proteins present in these complexes were identified by mass spectrometry after separation by SDS-PAGE (the amount of complex that was loaded on the gel is listed in parentheses). The presence of a protein in the individual complex preparations is indicated by a number, which represents the absolute number of peptides sequenced for that protein. Note that several proteins were detected in multiple bands. If only one peptide has been identified for a given protein in a preparation, the score for this peptide is given in parentheses. Proteins previously identified in the two independent MS2 affinity selections of B complexes assembled in the absence of any inhibitor (Deckert et al. 2006), called here $B^{\#1}$ and $B^{\#2}$, are indicated with the numbers of peptides sequenced for each protein as explained above. Calculated molecular masses and accession numbers in the GenBank database at the NCBI are indicated. The gene names of the *S. cerevisiae* and *S. pombe* homologs of the indicated human protein are given. A question mark indicates that it is currently not clear whether the indicated yeast protein is a true functional homolog. BLAST alignments of both p68 (DDX5) and p72 (DDX17) revealed significant homology with *S. cerevisiae DBP2* and *S. pombe dbp2* (between 56% and 59% sequence identity, respectively). Since true homology remains to be verified, *DBP2* and *dbp2* are both enclosed in parentheses.

found to be associated predominately with C complexes (Bessonov et al. 2008), is clearly present in the B^{DHC} and $B^{splitomicin}$ complexes.

6. Peptides derived from all proteins of the hPRP19/CDC5 complex and (with the exception of PRCC in the B^{BA3} complex) from all hPRP19/CDC5 complex-related factors were found in the stalled spliceosomes, indicating that the incorporation of this complex into the spliceosome is not blocked by any of the inhibitors. However, the number of peptides derived from Npw38BP and Npw38 was higher in B^{BA3} than in the other B complexes. Moreover, the number of sequenced peptides derived from hECM2 (fSAP47) was drastically increased in the B^{DHC} and $B^{splitomicin}$ complexes as compared with other stalled B complexes (and also to the native B complex).
7. Inspection of the non-snRNP proteins shows additional characteristic peptide patterns for the various stalled B complexes. The kinase CDK11 (CDC2L2) that was previously detected in complex A (Behzadnia et al. 2006) is also found in the B^{BA3} complex, but not in any other B complex. In general, it seems that B^{BA3} contains more of the proteins that were previously detected in complex A as compared with the other stalled B complexes. Moreover, in B^{BA3} the number of peptides derived from GCIP p29, hSmu-1 (fSAP57), and RED proteins were significantly increased, whereas in B^{SAHA} complexes GCIPp29 was detected by only one peptide, and the number of peptides derived from hSmu-1 and RED was lower as in the other stalled (but not in the native) B complexes. Furthermore, B^{SAHA} did not contain the p68 DExD/H box helicase, which could be identified in all the other stalled B complexes.
8. Another difference is that hPrp17 was clearly detectable in B^{BA3} and B^{SAHA} complexes with a surprisingly large number of peptides (22 and 26, respectively).

Taken together, there are clear differences in the protein patterns of the stalled spliceosomes as determined by mass spectrometry, both among the stalled spliceosomes and between these and the previously characterized native A and B complexes. This indicates that the splicing cycle is blocked at distinct stages by the different novel inhibitors of pre-mRNA splicing, and that these stages have not been previously observed.

DISCUSSION

Here, we show that three inhibitors of protein deacetylation as well as three inhibitors of protein acetylation interfere with pre-mRNA splicing in vitro. As defined by the U snRNA-composition of the stalled spliceosomes, two HAT inhibitors allow only the formation of A-like splicing complexes, while in the presence of the three HDAC inhibitors and a third HAT inhibitor, B-type spliceosomes can still be assembled, albeit without the capacity for becoming activated for catalysis. The protein compositions showed that the stalled complexes differ from each other and from the normal (i.e., not stalled) A and B complexes.

Inhibition of pre-mRNA splicing by inhibitors of protein acetylation and deacetylation

We initially chose to test inhibitors of protein acetylation and deacetylation regarding their effect on pre-mRNA splicing in part, because the corresponding deacetylating enzymes have been previously identified in purifications of mixtures of splicing complexes (Rappsilber et al. 2002; Zhou et al. 2002). The presence of such enzymatic functions, our finding that both the U2- and the U12-dependent splicing pathways are indeed blocked by inhibitors of HATs and HDACs, and the failure of non-inhibitory derivatives to stall splicing, together suggest that acetylation and deacetylation of spliceosomal proteins and the activity of the corresponding spliceosomal enzymes may be required for pre-mRNA splicing.

It was surprising that for the SAHA-related HDAC inhibitors the IC_{50} for inhibition of pre-mRNA splicing turned out to be some three orders of magnitude higher than in standard deacetylation assays. This may perhaps be attributed to local structural differences between the various deacetylation enzymes to which these inhibitors bind. Another possible explanation is that these compounds are unstable in the nuclear extract, so that only a small fraction remains active in inhibiting pre-mRNA splicing. For two inhibitors of the NAD-dependent HDACs (DHC and splitomicin), we found IC_{50} values for inhibition of pre-mRNA splicing that were only slightly higher than for standard deacetylation reactions. Unexpectedly, nicotinamide—considered to be a competitive inhibitor for all NAD-dependent deacetylases (Bitterman et al. 2002)—had no effect on pre-mRNA splicing, which raises the question of the mechanism by which DHC and splitomicin stall the splicing reaction. Since the inhibition of NAD-dependent HDACs can apparently overlap with that of protein kinases (Trapp et al. 2006), it is conceivable that DHC and splitomicin interfere with a spliceosomal kinase rather than an HDAC block pre-mRNA splicing. Further work is required to find out whether the spliceosome's target for DHC or splitomicin is, in fact, an HDAC or another enzyme.

The three HAT inhibitors investigated—AA, BA3, and garcinol—blocked pre-mRNA splicing with similar IC_{50} values as observed for the acetylation of proteins. However, they differed in an important respect: while AA and garcinol—reported to inhibit both the p300/CBP and Gcn5/PCAF families of HATs (Balasubramanyam et al. 2003, 2004)—only allow the formation of A-like splicing complexes, BA3—specific for the Gcn5/PCAF family of HATs (Biel et al. 2004)—blocks the splicing cycle after all five U snRNPs have been stably assembled on the

pre-mRNA. This may suggest that a p300/CBP-type enzyme is required for the formation of complex B formation, while a Gcn5/PCAF-like HAT functions during activation of the spliceosome after complex B has formed. However, to our knowledge, these three HAT inhibitors have only been analyzed in vitro in protein acetylation assays using purified components and have not been tested regarding their effect on other enzymes.

A role of HDACs and HATs in the splicing of pre-mRNA would require one or more spliceosomal protein(s) to become acetylated during the reaction. Initial experiments to detect acetylated splicing factors (e.g., immunoblotting using antibodies against acetylated lysine side chains, or splicing in vitro in the presence of radioactively labeled acetyl-coenzyme A) were not successful. However, this is not surprising, partly because it is not known whether the spliceosomal proteins that are acetylated are present in the purified complexes as used in these attempts: a number of proteins known to be splicing factors, such as RNA helicases or protein kinases, interact only transiently with spliceosomal complexes and are thus absent from purified spliceosomes. Additional experiments, beyond the scope of this study, will be required to identify the site(s) of acetylation and thus provide detailed confirmation of the part played by it in the splicing cycle.

Differences in protein composition among splicing complexes: Stalled and native

Our RNA analyses and centrifugation results show that the stalled splicing complexes are associated with distinct steps of the splicing cycle. We therefore determined their respective proteomes by mass spectrometry; of particular interest was the comparison with native A and B complexes as described earlier (Deckert et al. 2006; Behzadnia et al. 2007). As in our previous studies, we followed the absolute number of sequenced peptides derived from the corresponding proteins. Although not strictly quantitative, the number of sequenced peptides can be indicative of the amount of a protein in the sample; such correlations were found in our previous studies when tested by immunoblotting (Makarov et al. 2002; Makarova et al. 2004; Behzadnia et al. 2007; Bessonov et al. 2008), and have been recently described in detail (Rappsilber et al. 2002; Ishihama et al. 2005).

The A complexes stalled by AA and garcinol contained a significantly lower number of proteins than the native A complex as described by Behzadnia et al. (2007). A complexes assembled in the presence of garcinol contained mainly 17S U2 snRNP and related proteins (with larger numbers of sequenced peptides derived from hPrp43 and SR140). The U1 snRNP-specific proteins were hardly detectable by mass spectrometry (one peptide derived from U1 70K and three peptides derived from U1 A), and U1 snRNP-related proteins were completely absent. Almost no other proteins (except for NFAR and NF 45 proteins, see below) were detected: those absent thus included the SR and hnRNP proteins, hPrp19/CDC5 and related proteins, as well as other proteins previously detected in A and B complexes. A similar tendency was seen for the A^{AA} complex: although U1 snRNP proteins were still identified by a significant number of sequenced peptides, the two proteins functionally linked to the U1 snRNP—FBP11 and S164, the human homologs of the yeast U1 snRNP proteins Prp40 and Snu71 (Kao and Siliciano 1996; Gottschalk et al. 1998)—were also absent. The reduction in U1 snRNP proteins in stalled (compared with native) A complexes seems to coincide with a reduction in the SR proteins as seen by the reduced numbers of sequenced SR peptides. It is important to point out that greater amounts of the stalled A complexes were found by mass spectrometry compared with the native A complex. More protein input is expected to give rise to a larger number of peptides identified. This makes the absence or under-representation of any protein in the stalled A complexes even more significant.

We observed numerous sequenced peptides derived from NFAR and NF45 in the two stalled A complexes. NFAR and NF45 are RNA-binding proteins previously described in the replication of positive-strand RNA viruses (Isken et al. 2003), and they have also been found in spliced mRNPs (Merz et al. 2007). Further experiments will be needed to show whether these, and perhaps other, proteins play a direct part in pre-mRNA splicing. Moreover, the mechanism of the failure to assemble complex B will have to be confirmed; although the tacit assumption that the stalling takes place because a catalytic function of complex A is inhibited is a reasonable one, the alternative possibility that the inhibitors act on the tri-snRNP—or another protein (-complex) required at this point of the splicing cycle—rather than on complex A cannot be excluded. Likewise, the effect of the small-molecule inhibitors could theoretically be related not to their inhibition of an enzymatic activity, but instead to some other effect such as the steric blockage of an essential docking process.

The differences between the native B complex and the individual stalled B complexes (and also among the stalled spliceosomes themselves) are more subtle than the differences between the native A and the A^{AA} and $A^{garcinol}$ complexes. Nonetheless, by comparing the numbers of peptides obtained from the stalled B complexes with numbers from the native complex B (where almost stoichiometric amounts of all the U snRNPs, including U1 snRNP, are expected), it is obvious that U1 snRNP proteins are under-represented in the B^{SAHA}, B^{DHC}, and $B^{splitomicin}$ complexes (Table 3). As seen for the stalled A complexes, the reduction of U1 snRNP proteins and the complete absence of the U1 snRNP-related proteins FBP11 and S164 coincide with a decrease in the number of peptides derived from SR proteins. The finding that the U1 snRNP can apparently dissociate from the spliceosome, while the U4 snRNA remains stably bound, is interesting, because it was

previously proposed that these two U snRNPs are released during activation of the spliceosome in a coupled manner (Kuhn et al. 1999; Staley and Guthrie 1999). However, in the presence of the HDAC inhibitors SAHA, splitomicin, or DHC, these events are seemingly uncoupled. The low level of U1 snRNA and U1 snRNP proteins detected by silver staining and mass spectrometry, respectively, is probably due to the presence of splicing complexes that have not yet completely reached the stage of being blocked by the inhibitors. Simple loss of the U1 snRNP and related proteins during the purification can be excluded, because apparently stoichiometric amounts of U1 snRNA are found in B^{BA3} as shown in this study and in the native B complex (Deckert et al. 2006).

The larger numbers of sequenced peptides of U1 snRNP-specific and -associated factors in the B^{BA3} complex suggest that the block by BA3 takes place at an earlier stage of B-complex formation than that blocked by the other three inhibitors. Overall, the B^{BA3} complex has the most complex proteome, with several proteins showing an increased number of sequenced peptides as compared with other B complexes. These were hPrp43, SPF45, TFIP11, Npw38BP, Npw38, CDK11 (CDC2l2), HCNPG, GCIPp29, hSmu-1 (fSAP57), RED, and hPrp17. TFIP11 is the human homolog of yeast Spp382/Ntr1, which has been shown to interact with yeast Prp43 (Lebaron et al. 2005; Tsai et al. 2005; Boon et al. 2006; Pandit et al. 2006). The observed increase in the numbers of sequenced peptides of both proteins is consistent with their functional and structural interaction. In addition, the presence of both proteins in the B^{BA3} complex suggests that these two function at a step during the splicing cycle that takes place after addition of the tri-snRNP and the hPRP19/CDC5 complex to the spliceosome, but before the release of the U1 snRNP. A similar argument can be made for other B^{BA3} complex-specific factors such as the kinase CDK11 (CDC2L2), which has been implicated in pre-mRNA splicing (Hu et al. 2003). While further work will be required to elucidate the functions of these splicing factors in detail, a first classification can be made on the basis of the data presented here. This may be expected to help in the design of future studies to examine the roles of these splicing factors.

Small-molecule inhibitors of pre-mRNA splicing as a tool to study spliceosome structure and function

Small molecules have already been used in studying pre-mRNA splicing. For example, inhibitors of protein kinases and phosphatases have been used to study the role of protein phosphorylation in pre-mRNA splicing (Mermoud et al. 1992; Parker and Steitz 1997). Using splicing reactions in vitro, Soret et al. (2005) screened 4000 compounds and found that indole derivatives interact directly with selected members of SR proteins—key modulators of alternative splicing. Two small molecules that modulate pre-mRNA splicing were reported recently (Kaida et al. 2007; Kotake et al. 2007); both target the splicing factor SF3b of the 17S U2 snRNP.

In the experiments described in this study, we tested a limited set of compounds and were able to identify inhibitors that block the reaction at different points of the splicing cycle. This allowed us to block the splicing cycle at a distinct step and then purify the stalled spliceosome for structural characterization.

To identify more inhibitors of pre-mRNA splicing that target the multitude of individual steps during the splicing cycle, it will be necessary to screen a larger number of compounds. This will be difficult to perform manually; thus, automation of the splicing reaction in vitro will be required.

The success seen in the studies regarding small-molecule inhibitors of pre-mRNA splicing as published so far suggests that additional compounds that influence the splicing reaction are likely to be identified in the future. These will be valuable tools for a detailed structural and functional analysis of the spliceosome.

MATERIALS AND METHODS

Splicing substrates, reactions, and spliceosome complex analysis

A transcription template for the MINX pre-mRNA was generated from the pMINX plasmid (Zillmann et al. 1988) by PCR. A PCR product containing three MS2 coat protein RNA-binding sites was generated using pAdML-M3 (Zhou et al. 2002), which was a kind gift from R. Reed. A transcription template for MINX pre-mRNA tagged with three MS2 aptamers at the 3′-end of exon2 (MINX-M3) was generated by overlapping PCR of the MINX and MS2 PCR products. Plasmid pP120 (Tarn and Steitz 1996) was linearized with HindIII for use as a template in transcribing p120 pre-mRNA. Uniformly ^{32}P-labeled, m^{7}G(5′)ppp(5′)G-capped pre-mRNA was synthesized in vitro by T7 runoff transcription.

HeLa nuclear extract was prepared according to Dignam et al. (1983). Splicing reactions with U2-dependent pre-mRNAs contained 40% (v/v) HeLa nuclear extract in buffer D [20 mM HEPES-KOH at pH 7.9, 100 mM KCl, 1.5 mM $MgCl_2$, 0.2 mM EDTA, 20% (v/v) glycerol, 0.5 mM DTT, 0.5 mM PMSF], 25 mM KCl, 3 mM $MgCl_2$, 20 mM creatine phosphate, 2 mM ATP, 3 nM ^{32}P-labeled pre-mRNA, 5% (v/v) DMSO, and the indicated concentration of the chemicals tested for their effect on splicing. The nuclear extract was pre-incubated with the chemical (or just DMSO as a control) for 10 min at 30°C, and the reactions were then started by addition of the other components. For the analysis of the splicing products, the reactions were stopped after 90 min; RNA was isolated by proteinase K treatment, phenol extraction, and ethanol precipitation; separated by denaturing polyacrylamide gel electrophoresis on an 8.3 M urea/14% (w/v) polyacrylamide gel; and visualized by autoradiography. Amounts of RNA were measured with a PhosphorImager (Molecular Dynamics). Splicing efficiency was calculated by the ratio [mRNA]/([mRNA]+[pre-mRNA]) and expressed as a percentage of the corresponding ratio for the control reaction with DMSO. For the analysis of the spliceosomal complexes, 10 μL of the splicing reaction were added to 2.5 μL of loading buffer [1× TBE,

30% (v/v) glycerol, 1.25 μg/μL heparin] at the time points indicated, and then placed on ice. Complexes were separated on 2% (w/v) agarose gels (Das and Reed 1999).

Splicing of the U12-dependent p120 pre-mRNA in vitro was performed essentially as described above for the U2-dependent pre-mRNAs; the reaction time was 6 h, with 60% (v/v) HeLa nuclear extract, 4.8 μM of a 2′-*O*-methyl RNA oligonucleotide complementary to the U6 snRNA (5′-AUGCUAAUCUUCUCUG UA-3′) to inhibit U2-type splicing, 1.5% poly(vinyl alcohol), 3% or 5% (v/v) DMSO, and the indicated concentration of the respective chemical to be tested for its effect on splicing. RNA was recovered by phenol extraction and ethanol precipitation, fractionated on an 8.3 M urea/8% (w/v) polyacrylamide gel, and visualized by autoradiography.

MS2 affinity selection of stalled spliceosomal complexes

Stalled spliceosomal complexes were isolated under native conditions essentially as previously described (Deckert et al. 2006). Briefly, radioactively labeled MS2-tagged MINX pre-mRNA was first bound to a purified fusion protein of MS2 and maltose-binding protein (MS2-MBP). Next, a 12-mL splicing reaction was set up as described above, but containing 10 nM (for A-like spliceosomes) or 20 nM (for B-type splicing complexes) MS2-tagged MINX pre-mRNA along with 0.2 mM AA, 1.35 mM BA3, 0.15 mM garcinol, 3.75 mM SAHA, 2 mM splitomicin, or 5 mM DHC. Spliceosomal complexes were allowed to assemble for 30 min (garcinol, splitomicin, and DHC) or 60 min (AA, BA3, and SAHA) at 30°C. The reaction was then loaded onto 14-mL linear 5%–20% (v/v) (for the A-like splicing complexes) or 10%–30% (v/v) (for the B-like splicing complexes) glycerol gradients containing buffer G (20 mM HEPES-KOH at pH 7.9, 150 mM NaCl, 1.5 mM $MgCl_2$). Gradients were centrifuged for 16 h at 140,000*g* (for the A-like splicing complexes) or at 80,000*g* (for the B-like splicing complexes) in a Sorvall Tst 41.14 rotor, and harvested manually in 500-μL fractions. The distribution of ^{32}P-labeled pre-mRNA across the gradient was determined by Cherenkov counting, and peak fractions containing the stalled spliceosomal complexes were loaded onto a column of amylose beads (New England Biolabs) equilibrated with buffer G. After extensive washing, the stalled spliceosomal complexes were eluted dropwise with elution buffer (buffer G+12 mM maltose). RNA was isolated from the eluates by proteinase K treatment, phenol extraction, and ethanol precipitation, separated by denaturing polyacrylamide gel electrophoresis on an 8.3 M urea/10% (w/v) polyacrylamide gel, and visualized by staining with silver and autoradiography.

In vitro splicing assays with MS2 affinity-selected splicing complexes

U2-depleted HeLa nuclear extract was prepared by affinity selection with a biotinylated 2′-*O*-methyl RNA oligonucleotide complementary to nucleotides 1–20 of U2 snRNA (RNA-Tec) and streptavidin-agarose beads essentially as described previously (Behzadnia et al. 2006), except that the oligonucleotide was used at a concentration of 3 μM. HeLa nuclear extract was treated with micrococcal nuclease (MN) as described previously (Makarov et al. 2002). In vitro splicing (60 μL of reaction volume) was performed essentially as described above for 3 h with 10 μL of the amylose column eluates containing MS2 affinity-selected splicing complexes (~50 fmol), and 40% buffer D, 40% ΔU2 nuclear extract, or 40% MN-treated nuclear extract. To assay whether the active splicing complexes are formed de novo on the tagged MINX-M3 pre-mRNA during splicing complementation in the presence of either 40% ΔU2 or 40% MN-treated nuclear extract, an additional reaction with an equimolar amount of radioactive, untagged MINX pre-mRNA with identical specific activity was performed. In each case, the RNA was isolated as described above, separated on an 8.3 M urea/14% (w/v) polyacrylamide gel, and visualized by autoradiography.

Mass spectrometry

Proteins recovered from individual affinity-selected complexes were separated by 10%–13% SDS-PAGE and stained with Coomassie blue. An entire lane of the Coomassie-blue-stained gel was cut into approximately 70 slices, and proteins were digested in the gel with trypsin and extracted according to Shevchenko et al. (1996). The extracted peptides were analyzed in a liquid-chromatography-coupled electrospray ionization quadrupole time-of-flight mass spectrometer under standard conditions. Proteins were identified by searching fragment spectra of sequenced peptides against the NCBI nonredundant database using Mascot as a search engine, and scored according to Pappin et al. (1993).

ACKNOWLEDGMENTS

We are grateful to T. Conrad, P. Kempkes, and H. Kohansal for excellent technical assistance, and to M. Raabe and U. Plessmann for excellent help with mass-spectrometry analyses. M.A.v.S. was supported by the DAAD and the Graduate Program 521 of the Deutsche Forschungsgemeinschaft. This work was supported by grants from the EU (Eurasnet, contract No. 518238; 6th framework) and Volkswagenstiftung to R.L., and by HFSP grant RGY0056/2004 to A.S.

Received August 27, 2008; accepted October 15, 2008.

REFERENCES

Babic, I., Jakymiw, A., and Fujita, D.J. 2004. The RNA binding protein Sam68 is acetylated in tumor cell lines, and its acetylation correlates with enhanced RNA binding activity. *Oncogene* **23:** 3781–3789.

Balasubramanyam, K., Swaminathan, V., Ranganathan, A., and Kundu, T.K. 2003. Small molecule modulators of histone acetyltransferase p300. *J. Biol. Chem.* **278:** 19134–19140.

Balasubramanyam, K., Altaf, M., Varier, R.A., Swaminathan, V., Ravindran, A., Sadhale, P.P., and Kundu, T.K. 2004. Polyisoprenylated benzophenone, garcinol, a natural histone acetyltransferase inhibitor, represses chromatin transcription and alters global gene expression. *J. Biol. Chem.* **279:** 33716–33726.

Bedalov, A., Gatbonton, T., Irvine, W.P., Gottschling, D.E., and Simon, J.A. 2001. Identification of a small molecule inhibitor of Sir2p. *Proc. Natl. Acad. Sci.* **98:** 15113–15118.

Behzadnia, N., Hartmuth, K., Will, C.L., and Lührmann, R. 2006. Functional spliceosomal A complexes can be assembled in vitro in the absence of a penta-snRNP. *RNA* **12:** 1738–1746.

Behzadnia, N., Golas, M.M., Hartmuth, K., Sander, B., Kastner, B., Deckert, J., Dube, P., Will, C.L., Urlaub, H., Stark, H., et al. 2007. Composition and three-dimensional EM structure of double affinity-purified, human prespliceosomal A complexes. *EMBO J.* **26:** 1737–1748.

Bessonov, S., Anokhina, M., Will, C.L., Urlaub, H., and Lührmann, R. 2008. Isolation of an active step I spliceosome and composition of its RNP core. *Nature* **452:** 846–850.

Biel, M., Kretsovali, A., Karatzali, E., Papamatheakis, J., and Giannis, A. 2004. Design, synthesis, and biological evaluation of a small-molecule inhibitor of the histone acetyltransferase Gcn5. *Angew. Chem. Int. Ed. Engl.* **43:** 3974–3976.

Bitterman, K.J., Anderson, R.M., Cohen, H.Y., Latorre-Esteves, M., and Sinclair, D.A. 2002. Inhibition of silencing and accelerated aging by nicotinamide, a putative negative regulator of yeast Sir2 and human SIRT1. *J. Biol. Chem.* **277:** 45099–45107.

Blencowe, B.J. 2006. Alternative splicing: New insights from global analyses. *Cell* **126:** 37–47.

Boon, K.L., Auchynnikava, T., Edwalds-Gilbert, G., Barrass, J.D., Droop, A.P., Dez, C., and Beggs, J.D. 2006. Yeast Ntr1/Spp382 mediates Prp43 function in postspliceosomes. *Mol. Cell. Biol.* **26:** 6016–6023.

Cleary, J., Sitwala, K.V., Khodadoust, M.S., Kwok, R.P., Mor-Vaknin, N., Cebrat, M., Cole, P.A., and Markovitz, D.M. 2005. p300/CBP-associated factor drives DEK into interchromatin granule clusters. *J. Biol. Chem.* **280:** 31760–31767.

Das, R. and Reed, R. 1999. Resolution of the mammalian E complex and the ATP-dependent spliceosomal complexes on native agarose mini-gels. *RNA* **5:** 1504–1508.

Deckert, J., Hartmuth, K., Boehringer, D., Behzadnia, N., Will, C.L., Kastner, B., Stark, H., Urlaub, H., and Lührmann, R. 2006. Protein composition and electron microscopy structure of affinity-purified human spliceosomal B complexes isolated under physiological conditions. *Mol. Cell. Biol.* **26:** 5528–5543.

Dignam, J.D., Lebovitz, R.M., and Roeder, R.G. 1983. Accurate transcription initiation by RNA polymerase II in a soluble extract from isolated mammalian nuclei. *Nucleic Acids Res.* **11:** 1475–1489.

Gottschalk, A., Tang, J., Puig, O., Salgado, J., Neubauer, G., Colot, H.V., Mann, M., Seraphin, B., Rosbash, M., Lührmann, R., et al. 1998. A comprehensive biochemical and genetic analysis of the yeast U1 snRNP reveals five novel proteins. *RNA* **4:** 374–393.

Grozinger, C.M. and Schreiber, S.L. 2002. Deacetylase enzymes: Biological functions and the use of small-molecule inhibitors. *Chem. Biol.* **9:** 3–16.

Grozinger, C.M., Chao, E.D., Blackwell, H.E., Moazed, D., and Schreiber, S.L. 2001. Identification of a class of small molecule inhibitors of the sirtuin family of NAD-dependent deacetylases by phenotypic screening. *J. Biol. Chem.* **276:** 38837–38843.

Hartmuth, K., Urlaub, H., Vornlocher, H.P., Will, C.L., Gentzel, M., Wilm, M., and Lührmann, R. 2002. Protein composition of human prespliceosomes isolated by a tobramycin affinity-selection method. *Proc. Natl. Acad. Sci.* **99:** 16719–16724.

Hastings, M.L. and Krainer, A.R. 2001. Pre-mRNA splicing in the new millennium. *Curr. Opin. Cell Biol.* **13:** 302–309.

Hildmann, C., Riester, D., and Schwienhorst, A. 2007. Histone deacetylases—An important class of cellular regulators with a variety of functions. *Appl. Microbiol. Biotechnol.* **75:** 487–497.

Hu, D., Mayeda, A., Trembley, J.H., Lahti, J.M., and Kidd, V.J. 2003. CDK11 complexes promote pre-mRNA splicing. *J. Biol. Chem.* **278:** 8623–8629.

Imai, S., Armstrong, C.M., Kaeberlein, M., and Guarente, L. 2000. Transcriptional silencing and longevity protein Sir2 is an NAD-dependent histone deacetylase. *Nature* **403:** 795–800.

Ishihama, Y., Oda, Y., Tabata, T., Sato, T., Nagasu, T., Rappsilber, J., and Mann, M. 2005. Exponentially modified protein abundance index (emPAI) for estimation of absolute protein amount in proteomics by the number of sequenced peptides per protein. *Mol. Cell. Proteomics* **4:** 1265–1272.

Isken, O., Grassmann, C.W., Sarisky, R.T., Kann, M., Zhang, S., Grosse, F., Kao, P.N., and Behrens, S.E. 2003. Members of the NF90/NFAR protein group are involved in the life cycle of a positive-strand RNA virus. *EMBO J.* **22:** 5655–5665.

Jurica, M.S. and Moore, M.J. 2003. Pre-mRNA splicing: Awash in a sea of proteins. *Mol. Cell* **12:** 5–14.

Jurica, M.S., Licklider, L.J., Gygi, S.R., Grigorieff, N., and Moore, M.J. 2002. Purification and characterization of native spliceosomes suitable for three-dimensional structural analysis. *RNA* **8:** 426–439.

Kaida, D., Motoyoshi, H., Tashiro, E., Nojima, T., Hagiwara, M., Ishigami, K., Watanabe, H., Kitahara, T., Yoshida, T., Nakajima, H., et al. 2007. Spliceostatin A targets SF3b and inhibits both splicing and nuclear retention of pre-mRNA. *Nat. Chem. Biol.* **3:** 576–583.

Kao, H.Y. and Siliciano, P.G. 1996. Identification of Prp40, a novel essential yeast splicing factor associated with the U1 small nuclear ribonucleoprotein particle. *Mol. Cell. Biol.* **16:** 960–967.

Kotake, Y., Sagane, K., Owa, T., Mimori-Kiyosue, Y., Shimizu, H., Uesugi, M., Ishihama, Y., Iwata, M., and Mizui, Y. 2007. Splicing factor SF3b as a target of the antitumor natural product pladienolide. *Nat. Chem. Biol.* **3:** 570–575.

Kouzarides, T. 2000. Acetylation: A regulatory modification to rival phosphorylation? *EMBO J.* **19:** 1176–1179.

Krawczak, M., Reiss, J., and Cooper, D.N. 1992. The mutational spectrum of single base-pair substitutions in mRNA splice junctions of human genes: Causes and consequences. *Hum. Genet.* **90:** 41–54.

Kuhn, A.N., Li, Z., and Brow, D.A. 1999. Splicing factor Prp8 governs U4/U6 RNA unwinding during activation of the spliceosome. *Mol. Cell* **3:** 65–75.

Landry, J., Slama, J.T., and Sternglanz, R. 2000a. Role of NAD^+ in the deacetylase activity of the Sir2-like proteins. *Biochem. Biophys. Res. Commun.* **278:** 685–690.

Landry, J., Sutton, A., Tafrov, S.T., Heller, R.C., Stebbins, J., Pillus, L., and Sternglanz, R. 2000b. The silencing protein Sir2 and its homologs are NAD-dependent protein deacetylases. *Proc. Natl. Acad. Sci.* **97:** 5807–5811.

Lebaron, S., Froment, C., Fromont-Racine, M., Rain, J.C., Monsarrat, B., Caizergues-Ferrer, M., and Henry, Y. 2005. The splicing ATPase Prp43p is a component of multiple preribosomal particles. *Mol. Cell. Biol.* **25:** 9269–9282.

Liu, Z.R. 2002. p68 RNA helicase is an essential human splicing factor that acts at the U1 snRNA-5′ splice site duplex. *Mol. Cell. Biol.* **22:** 5443–5450.

Luo, J., Nikolaev, A.Y., Imai, S., Chen, D., Su, F., Shiloh, A., Guarente, L., and Gu, W. 2001. Negative control of p53 by Sir2α promotes cell survival under stress. *Cell* **107:** 137–148.

Makarov, E.M., Makarova, O.V., Urlaub, H., Gentzel, M., Will, C.L., Wilm, M., and Lührmann, R. 2002. Small nuclear ribonucleoprotein remodeling during catalytic activation of the spliceosome. *Science* **298:** 2205–2208.

Makarova, O.V., Makarov, E.M., Urlaub, H., Will, C.L., Gentzel, M., Wilm, M., and Lührmann, R. 2004. A subset of human 35S U5 proteins, including Prp19, function prior to catalytic step 1 of splicing. *EMBO J.* **23:** 2381–2391.

Martinez, E., Palhan, V.B., Tjernberg, A., Lymar, E.S., Gamper, A.M., Kundu, T.K., Chait, B.T., and Roeder, R.G. 2001. Human STAGA complex is a chromatin-acetylating transcription coactivator that interacts with pre-mRNA splicing and DNA damage-binding factors in vivo. *Mol. Cell. Biol.* **21:** 6782–6795.

Matter, N., Herrlich, P., and König, H. 2002. Signal-dependent regulation of splicing via phosphorylation of Sam68. *Nature* **420:** 691–695.

Mermoud, J.E., Cohen, P., and Lamond, A.I. 1992. Ser/Thr-specific protein phosphatases are required for both catalytic steps of pre-mRNA splicing. *Nucleic Acids Res.* **20:** 5263–5269.

Merz, C., Urlaub, H., Will, C.L., and Lührmann, R. 2007. Protein composition of human mRNPs spliced in vitro and differential requirements for mRNP protein recruitment. *RNA* **13:** 116–128.

Olaharski, A.J., Rine, J., Marshall, B.L., Babiarz, J., Zhang, L., Verdin, E., and Smith, M.T. 2005. The flavoring agent dihydrocoumarin reverses epigenetic silencing and inhibits sirtuin deacetylases. *PLoS Genet.* **1:** e77. doi: 10.1371/journal.pgen.0010077.

Pandit, S., Lynn, B., and Rymond, B.C. 2006. Inhibition of a spliceosome turnover pathway suppresses splicing defects. *Proc. Natl. Acad. Sci.* **103:** 13700–13705.

Pappin, D.J., Hojrup, P., and Bleasby, A.J. 1993. Rapid identification of proteins by peptide-mass fingerprinting. *Curr. Biol.* **3:** 327–332.

Parker, A.R. and Steitz, J.A. 1997. Inhibition of mammalian spliceosome assembly and pre-mRNA splicing by peptide inhibitors of protein kinases. *RNA* **3:** 1301–1312.

Rappsilber, J., Ryder, U., Lamond, A.I., and Mann, M. 2002. Large-scale proteomic analysis of the human spliceosome. *Genome Res.* **12:** 1231–1245.

Saito, A., Yamashita, T., Mariko, Y., Nosaka, Y., Tsuchiya, K., Ando, T., Suzuki, T., Tsuruo, T., and Nakanishi, O. 1999. A synthetic inhibitor of histone deacetylase, MS-27-275, with marked in vivo antitumor activity against human tumors. *Proc. Natl. Acad. Sci.* **96:** 4592–4597.

Shevchenko, A., Wilm, M., Vorm, O., and Mann, M. 1996. Mass spectrometric sequencing of proteins silver-stained polyacrylamide gels. *Anal. Chem.* **68:** 850–858.

Soares, L.M., Zanier, K., Mackereth, C., Sattler, M., and Valcarcel, J. 2006. Intron removal requires proofreading of U2AF/3′ splice site recognition by DEK. *Science* **312:** 1961–1965.

Soret, J., Bakkour, N., Maire, S., Durand, S., Zekri, L., Gabut, M., Fic, W., Divita, G., Rivalle, C., Dauzonne, D., et al. 2005. Selective modification of alternative splicing by indole derivatives that target serine-arginine-rich protein splicing factors. *Proc. Natl. Acad. Sci.* **102:** 8764–8769.

Staley, J.P. and Guthrie, C. 1998. Mechanical devices of the spliceosome: Motors, clocks, springs, and things. *Cell* **92:** 315–326.

Staley, J.P. and Guthrie, C. 1999. An RNA switch at the 5′ splice site requires ATP and the DEAD box protein Prp28p. *Mol. Cell* **3:** 55–64.

Stoilov, P., Lin, C.H., Damoiseaux, R., Nikolic, J., and Black, D.L. 2008. A high-throughput screening strategy identifies cardiotonic steroids as alternative splicing modulators. *Proc. Natl. Acad. Sci.* **105:** 11218–11223.

Su, G.H., Sohn, T.A., Ryu, B., and Kern, S.E. 2000. A novel histone deacetylase inhibitor identified by high-throughput transcriptional screening of a compound library. *Cancer Res.* **60:** 3137–3142.

Tarn, W.Y. and Steitz, J.A. 1996. A novel spliceosome containing U11, U12, and U5 snRNPs excises a minor class (AT-AC) intron in vitro. *Cell* **84:** 801–811.

Trapp, J., Jochum, A., Meier, R., Saunders, L., Marshall, B., Kunick, C., Verdin, E., Goekjian, P., Sippl, W., and Jung, M. 2006. Adenosine mimetics as inhibitors of NAD+-dependent histone deacetylases, from kinase to sirtuin inhibition. *J. Med. Chem.* **49:** 7307–7316.

Tsai, R.T., Fu, R.H., Yeh, F.L., Tseng, C.K., Lin, Y.C., Huang, Y.H., and Cheng, S.C. 2005. Spliceosome disassembly catalyzed by Prp43 and its associated components Ntr1 and Ntr2. *Genes & Dev.* **19:** 2991–3003.

Will, C.L. and Lührmann, R. 2006. Spliceosome structure and function. In *The RNA world III* (eds. R.F. Gesteland et al.), pp. 369–400. Cold Spring Harbor Laboratory Press, Cold Spring Harbor, NY.

Wilson, B.J., Bates, G.J., Nicol, S.M., Gregory, D.J., Perkins, N.D., and Fuller-Pace, F.V. 2004. The p68 and p72 DEAD box RNA helicases interact with HDAC1 and repress transcription in a promoter-specific manner. *BMC Mol. Biol.* **5:** 11. doi: 10.1186/1471-2199-5-11.

Yang, X.J. 2004. The diverse superfamily of lysine acetyltransferases and their roles in leukemia and other diseases. *Nucleic Acids Res.* **32:** 959–976.

Yoshida, M., Kijima, M., Akita, M., and Beppu, T. 1990. Potent and specific inhibition of mammalian histone deacetylase both in vivo and in vitro by trichostatin A. *J. Biol. Chem.* **265:** 17174–17179.

Zhou, Z., Licklider, L.J., Gygi, S.P., and Reed, R. 2002. Comprehensive proteomic analysis of the human spliceosome. *Nature* **419:** 182–185.

Zillmann, M., Zapp, M.L., and Berget, S.M. 1988. Gel electrophoretic isolation of splicing complexes containing U1 small nuclear ribonucleoprotein particles. *Mol. Cell. Biol.* **8:** 814–821.